

Elastic strain engineering of ferroic oxides

Darrell G. Schlom, Long-Qing Chen, Craig J. Fennie, Venkatraman Gopalan, David A. Muller, Xiaoqing Pan, Ramamoorthy Ramesh, and Reinhard Uecker

Using epitaxy and the misfit strain imposed by an underlying substrate, it is possible to elastically strain oxide thin films to percent levels—far beyond where they would crack in bulk. Under such strains, the properties of oxides can be dramatically altered. In this article, we review the use of elastic strain to enhance ferroics, materials containing domains that can be moved through the application of an electric field (ferroelectric), a magnetic field (ferromagnetic), or stress (ferroelastic). We describe examples of transmuting oxides that are neither ferroelectric nor ferromagnetic in their unstrained state into ferroelectrics, ferromagnets, or materials that are both at the same time (multiferroics). Elastic strain can also be used to enhance the properties of known ferroic oxides or to create new tunable microwave dielectrics with performance that rivals that of existing materials. Results show that for thin films of ferroic oxides, elastic strain is a viable alternative to the traditional method of chemical substitution to lower the energy of a desired ground state relative to that of competing ground states to create materials with superior properties.

The strain game

For at least 400 years, humans have studied the effects of pressure (hydrostatic strain) on the properties of materials.¹ In the 1950s, it was shown that biaxial strain, where a film is clamped to a substrate but free in the out-of-plane direction, can alter the transition temperatures of superconductors² (T_c) and ferroelectrics (T_C).³

What has changed in recent years is the magnitude of the biaxial strain that can be imparted. Bulk ferroic oxides are brittle and will crack under moderate strains, typically 0.1%. One way around this limitation is the approach of bulk crystal chemists, to apply “chemical pressure” through isovalent cation substitution. A disadvantage of such a bulk approach, however, is the introduction of disorder and potentially unwanted local distortions. Epitaxial strain, the trick of the thin-film alchemist, provides a potentially disorder-free route to large biaxial strain and has been used to greatly enhance the mobility of transistors^{4,5} (see the article by Bedell et al. in this issue), increase catalytic activity (see the article by Yildiz et

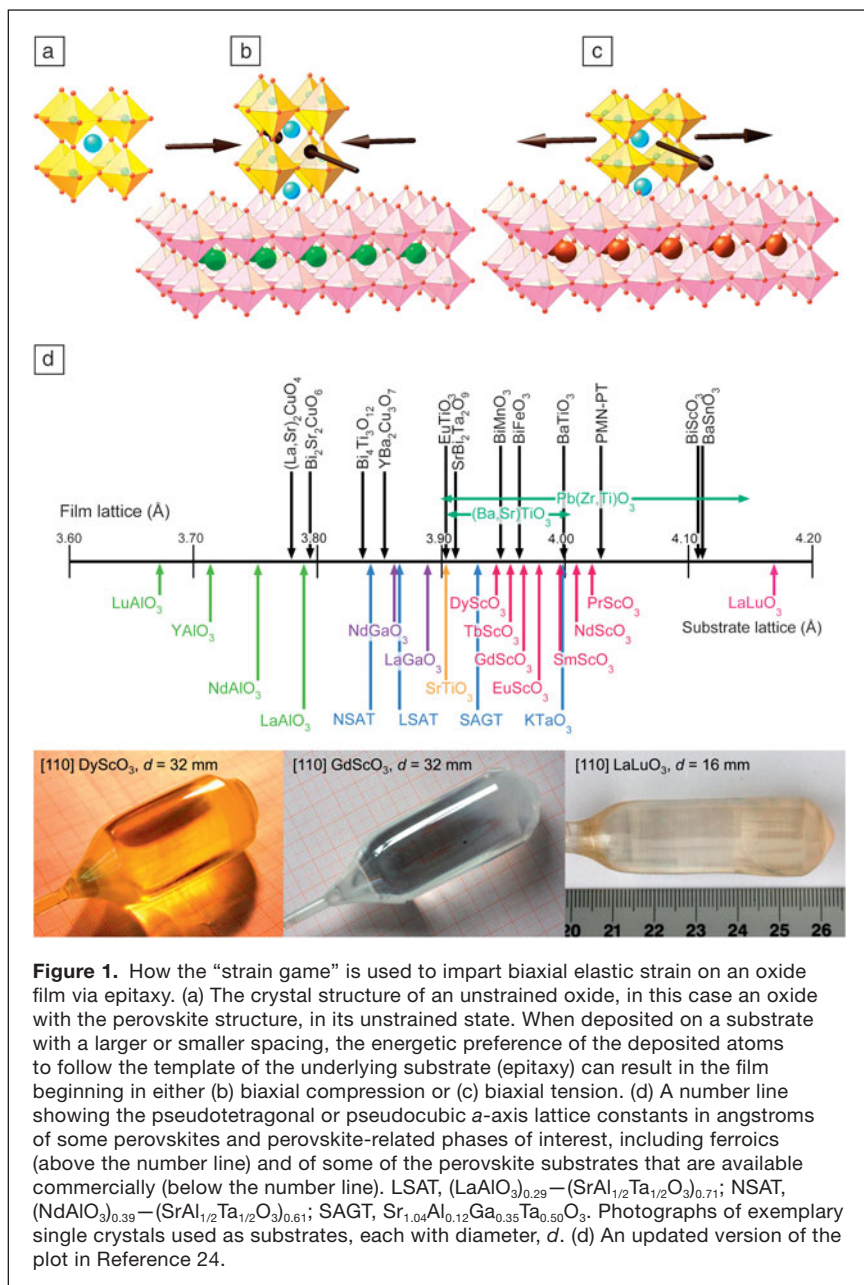
al in this issue), alter band structure⁶ (see the article by Yu et al. in this issue), and significantly increase superconducting,^{7,8} ferromagnetic,^{9–11} and ferroelectric^{12–16} transition temperatures. This approach, which we refer to as the “strain game,” is illustrated in **Figure 1** for elastically strained films of oxides with the perovskite structure.

Strains of about $\pm 3\%$ are common in epitaxial oxide films today,^{17–20} with the record to date being a whopping 6.6% compressive strain achieved in thin BiFeO₃ films grown on (110) YAlO₃.^{21–24} These strains are an order of magnitude higher than where these materials would crack in bulk.^{25–27}

Strained SrTiO₃ and the importance of suitable substrates

The strain game for ferroics was ignited by the demonstration that an oxide that normally is not ferroelectric at any temperature can be made ferroelectric at room temperature through the application of biaxial strain.¹² Such a gigantic shift in properties and T_C had never before been clearly seen in any

Darrell G. Schlom, Department of Materials Science and Engineering, Cornell University and Kavli Institute at Cornell for Nanoscale Science; schlom@cornell.edu
Long-Qing Chen, Millennium Science Complex, Materials Research Institute, Penn State University; lqc3@psu.edu
Craig J. Fennie, School of Applied and Engineering Physics, Cornell University; fennie@cornell.edu
Venkatraman Gopalan, Materials Science and Engineering, Penn State University; vgopalan@psu.edu
David A. Muller, School of Applied and Engineering Physics, Cornell University and Kavli Institute at Cornell for Nanoscale Science, Cornell; dm24@cornell.edu
Xiaoqing Pan, Department of Materials Science and Engineering, University of Michigan; panx@umich.edu
Ramamoorthy Ramesh, Oak Ridge National Laboratory; rameshr@ornl.gov
Reinhard Uecker, Leibniz Institute for Crystal Growth, Berlin; reinhard.uecker@ikz-berlin.de
DOI: 10.1557/mrs.2014.1

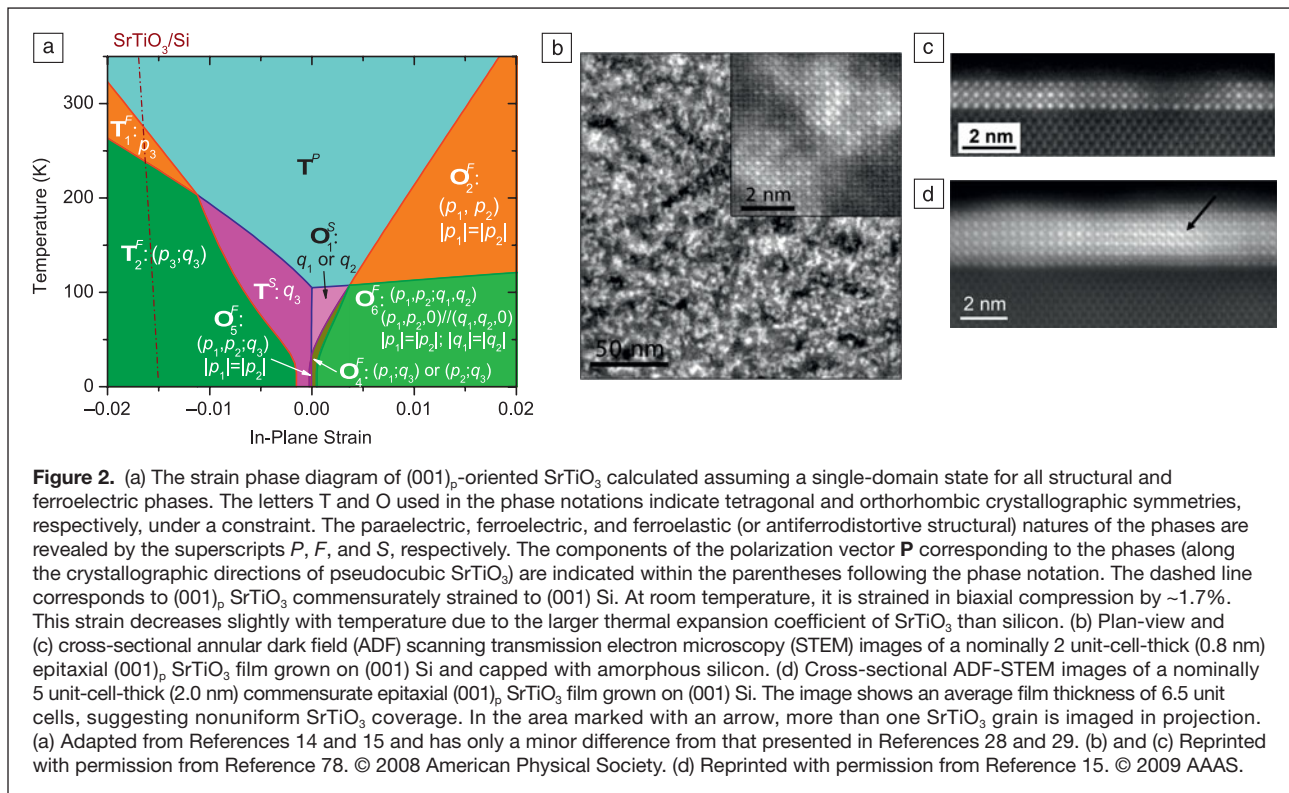


ferroic system; nonetheless, this achievement was the experimental realization of what had been predicted years earlier by theory.^{28,29} **Figure 2** shows the strain phase diagram of $(001)_p$ SrTiO_3 calculated by thermodynamic analysis,^{12,14,15,28–30} where the *p* subscript indicates pseudocubic Miller indices. These predictions imply that a biaxial tensile strain on the order of 1% will shift the T_C of SrTiO_3 to the vicinity of room temperature.^{12,28–32} Although many researchers had grown SrTiO_3 films on substrates with different spacings, the lattice mismatches were so large and the films so thick that the films were no longer elastically strained.

Fully commensurate, elastically strained epitaxial films have the advantage that high densities of threading dislocations

(e.g., the $\sim 10^{11}$ dislocations cm^{-2} observed, for example, in partially relaxed $(\text{Ba}_x\text{Sr}_{1-x})\text{TiO}_3$ films)^{33,34} are avoided. Strain fields around dislocations locally alter the properties of a film, making its ferroelectric properties inhomogeneous and often degraded.^{35–37} To achieve highly strained ferroic films and keep them free of such threading dislocations, one needs to keep them thin, typically not more than a factor of five beyond the Matthews-Blakeslee critical thickness, beyond which it becomes energetically favorable (though typically constrained by kinetics) for a film to relax by the introduction of dislocations.^{27,38} Thickness-dependent studies, involving the growth of a ferroic on just one substrate material to study the effect of strain in partially relaxed films, are not as easy to interpret as experiments utilizing commensurate films grown on several different substrate materials covering a range of lattice spacings. In the former, the strains are inhomogeneous, and the high concentration of threading dislocations can obfuscate intrinsic strain effects.

Exploring the strain predictions in Figure 2a was greatly simplified by the development of new substrates with a broad range of spacings to impart a desired strain state into the overlying SrTiO_3 film. These substrates have the same structure as SrTiO_3 —the perovskite structure—but different lattice spacings. The number of perovskite single crystals that are available commercially as large substrates (with surfaces at least $10 \text{ mm} \times 10 \text{ mm}$ in size) has nearly doubled in the last decade due to the work of the present authors.^{39–41} Today, various single crystal perovskite and perovskite-related substrates are commercially available (see Figure 1d), including LuAlO_3 ,^{42,43} YAlO_3 ,⁴⁴ LaSrAlO_4 ,⁴⁵ NdAlO_3 ,⁴⁶ LaAlO_3 ,^{47,48} LaSrGaO_4 ,⁴⁹ $(\text{NdAlO}_3)_{0.39} - (\text{SrAl}_{1/2}\text{Ta}_{1/2}\text{O}_3)_{0.61}$ (NSAT),⁵⁰ NdGaO_3 ,^{51,52} $(\text{LaAlO}_3)_{0.29} - (\text{SrAl}_{1/2}\text{Ta}_{1/2}\text{O}_3)_{0.71}$ (LSAT),^{50,53} LaGaO_3 ,⁵⁴ SrTiO_3 ,^{55–58} $\text{Sr}_{1.04}\text{Al}_{0.12}\text{Ga}_{0.35}\text{Ta}_{0.50}\text{O}_3$ (SAGT), DyScO_3 ,^{12,39} TbScO_3 ,⁴⁰ GdScO_3 ,^{13,39,59} EuScO_3 ,^{39,60} KTaO_3 ,⁶¹ NdScO_3 ,^{39,62} PrScO_3 ,⁶³ and LaLuO_3 ,⁶⁴ many of these are produced with structural perfection rivaling that of conventional semiconductors. The perfection of the substrate, the best of which are grown by the Czochralski method (which is not applicable to most ferroic oxides because they do not melt congruently), can be passed on to the film via epitaxy. This has led to the growth of strained epitaxial films of the ferroics SrTiO_3 ,^{38,65} BaTiO_3 ,¹⁴ BiFeO_3 ,⁶⁶ BiMnO_3 ,⁶⁷ and EuTiO_3 ,¹⁶ with rocking curve full width at half maximum values ≤ 11 arcsec (0.003°)—identical to those of the commercial substrates upon which they are grown and significantly narrower



(indicative of higher structural perfection) than the most perfect bulk single crystals of these same materials.

Using these new perovskite substrates, predictions of the SrTiO₃ strain phase diagram shown in Figure 2 were assessed. Not only was it found possible to transmute SrTiO₃ into a room temperature ferroic,^{12,68,69} but the experimentally determined point group,^{31,32,70–72} direction and magnitude of spontaneous polarization (P_S),^{31,32,65,70–73} observed shifts in T_C ^{12,70,71} and soft mode frequency with biaxial strain,⁷⁴ and existence of a transition to a simultaneously ferroelectric and ferroelastic phase at lower temperatures^{70–72,74} were all in accord with theory. Not all of the experimental observations, however, were in agreement with theory. For example, it was observed that strained SrTiO₃ films exhibit a significant frequency dependence to their dielectric response.^{65,73} This relaxor ferroelectric behavior is due to defects. On account of the strain, the SrTiO₃ matrix is highly polarizable and can be easily polarized by defect dipoles that arise from non-stoichiometry in the SrTiO₃ film. Based on how the properties of strained SrTiO₃ films vary with non-stoichiometry, strained, perfectly stoichiometric SrTiO₃ films are not expected to show relaxor behavior.⁷⁵

To make it possible for strain-enabled or strain-enhanced functionalities to be exploited in mainstream device architectures, it is desirable to play the strain game on substrates relevant to the semiconductor industry. One such example is the integration of commensurately strained SrTiO₃ films with silicon.¹⁵ The lattice mismatch between (001)_p SrTiO₃ and (001) Si is 1.7%, as indicated by the dashed line on the left side of the strain phase diagram in Figure 2a. From theory

(Figure 2a), such a film would be expected to be ferroelectric with a T_C near room temperature. This integration is, however, rather challenging due to (1) the high reactivity of silicon with many elements and their oxides,^{76,77} and (2) the thermodynamic driving force for a pristine silicon surface to oxidize and form an amorphous native oxide (SiO₂), which blocks epitaxy, under the oxidizing conditions typically used for the growth of oxide thin films. Despite these impediments, thin commensurate SrTiO₃ films have been grown directly on silicon without discernible intermediate layers and free of reaction, and are found to be ferroelectric at room temperature.¹⁵

Planar-view and cross-sectional annular dark field (ADF) scanning transmission electron micrographs (STEM) of epitaxial (001)_p SrTiO₃ films grown on and commensurately strained to (001) Si are shown in Figure 2b–d. Although the interface between SrTiO₃ and silicon is seen to be abrupt and free of reaction, these images reveal additional challenges to the growth of SrTiO₃ on silicon. First is the propensity of SrTiO₃ to nucleate as islands and not wet the surface of the silicon substrate.⁷⁸ Even using kinetically limited growth conditions,^{15,79} it takes multiple unit cells of growth before the SrTiO₃ islands coalesce.⁷⁸ Second are frequent out-of-phase boundaries in the SrTiO₃ film (see Figure 2d) resulting from the step height of (001) Si (0.14 nm) not matching the step height of (001)_p SrTiO₃ (0.39 nm). Out-of-phase boundaries can form during the coalescence of SrTiO₃ islands that have nucleated on different (001) Si terraces. The arrow in Figure 2d marks an area where the SrTiO₃ islands are out-of-phase with each other.

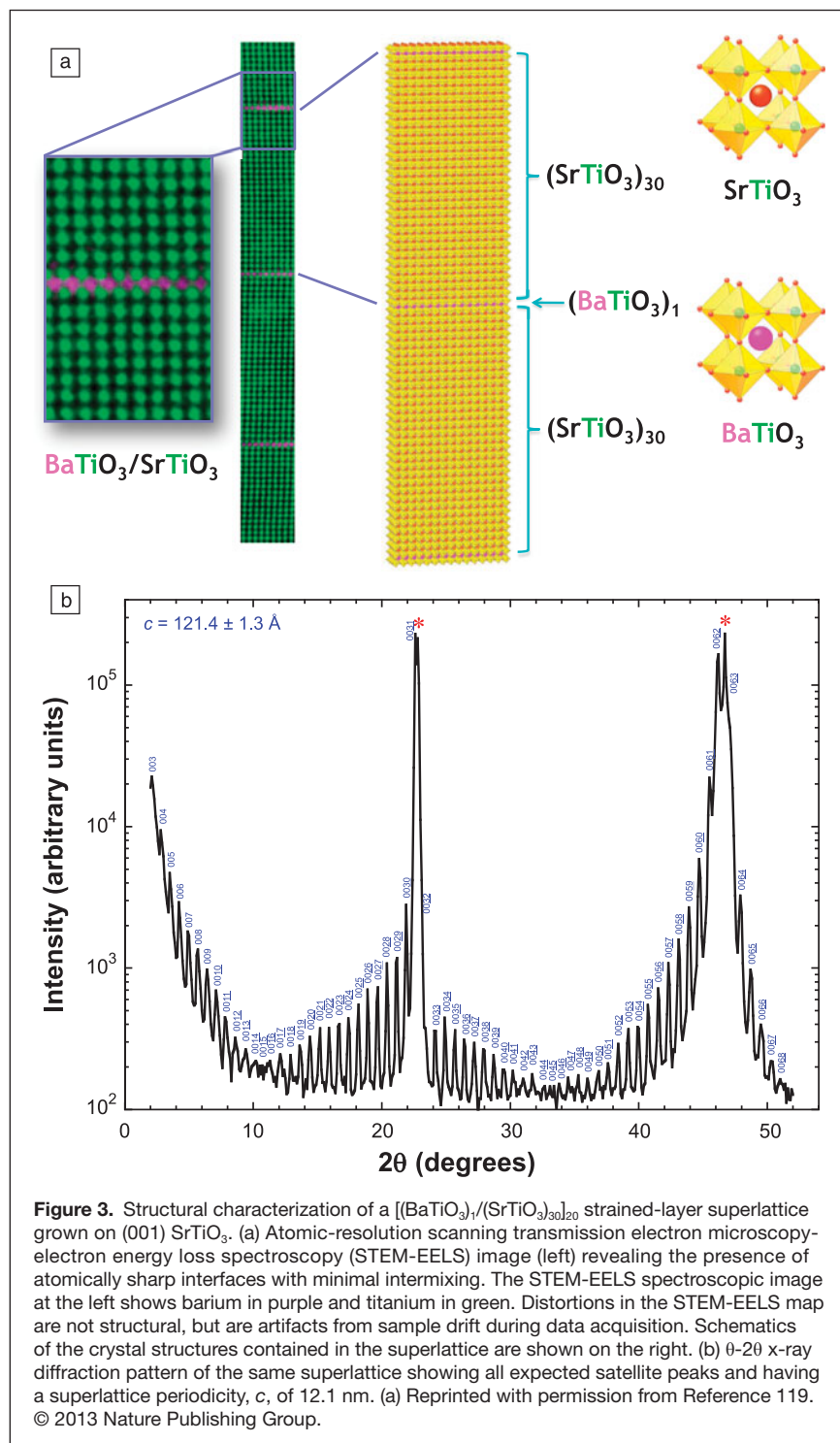
For the growth of high-quality films of ferroic oxides with a desired strain state, not only are appropriate substrates of exceptionally high perfection needed, but also methods to prepare them with smooth, well-ordered surfaces with a specific chemical termination on which epitaxial growth can be reliably initiated. For example, chemically polished (001) SrTiO₃ substrates display a mixture of SrO- and TiO₂-terminated surfaces.

A combination of chemical etching and annealing has been shown to yield SrTiO₃ substrates with known surface termination. Kawasaki et al.⁸⁰ showed that an NH₄F-buffered HF solution with controlled pH enables etching of the more basic SrO layer and leaves a completely TiO₂ terminated surface on the substrate. This method of preparing a TiO₂-terminated (001) SrTiO₃ surface has been further perfected by Koster et al.⁸¹ SrO-terminated (001) SrTiO₃ substrates can also be prepared.⁸² A means to prepare low defect surfaces with controlled termination has since been developed for (110) SrTiO₃,⁸³ (111) SrTiO₃,^{83,84} (001)_p LaAlO₃,^{85,86} (111)_p LaAlO₃,⁸⁵ (110) NdGaO₃,⁸⁶ (001)_p LSAT,^{86,87} (110) DyScO₃,^{88,89} (110) TbScO₃,⁸⁸ (110) GdScO₃,⁸⁸ (110) EuScO₃,⁸⁸ (110) SmScO₃,⁸⁸ (001) KTaO₃,⁹⁰ (110) NdScO₃,⁸⁸ and (110) PrScO₃.⁸⁸ substrates.

The strain game is capable of enhancing the properties of a multitude of ferroelectric systems. Shifts in ferroelectric T_c of roughly 300 K per percent biaxial strain, quite comparable to those predicted^{28–32} and observed^{12,68–74} for SrTiO₃, were first predicted by theory and subsequently verified by experiments on biaxially strained BaTiO₃^{13,14,91–94} and PbTiO₃^{14,91,95–100} films. Strain effects of comparable magnitude have also been observed in strained (Ba,Sr)TiO₃ films^{101,102} and in strained-layer superlattices: KTaO₃/KNbO₃,¹⁰³ SrTiO₃/SrZrO₃,¹⁰⁴ SrTiO₃/BaZrO₃,¹⁰⁵ PbTiO₃/SrTiO₃,^{106,107} BaTiO₃/SrTiO₃,^{108–111} and CaTiO₃/SrTiO₃/BaTiO₃.^{112–114}

The success of theory in predicting the effect of strain on a multitude of ferroelectrics, together with advances in the ability to customize the structure and strain of oxide heterostructures at the atomic-layer level, has enabled a new era: ferroelectric oxides by design.¹⁴ The appropriate theoretical methods to design strain-enhanced ferroelectrics depend on the material and whether or not domains need to be taken into account. First-principles methods are good for new materials where the coefficients of the Landau–Devonshire free energy expansion,³⁰ a Taylor expansion of the

free energy of a material in powers of its order parameter (polarization for typical ferroelectrics), are unknown. Due to the relatively small number of atoms that can be included in such calculations, however, the calculations are limited to single-domain materials. Measurements on materials can yield the coefficients needed in Landau–Devonshire thermodynamic analysis to calculate the effect of strain in the absence of domains.³⁰



Phase-field simulations, which also require coefficients obtained from either experiment or first-principles calculations, can be used to take domains into account.^{97,98} An example is $(\text{BaTiO}_3)_n/(\text{SrTiO}_3)_m$ strained-layer superlattices, where n and m refer to the thickness, in unit cells, of the $(001)_p$ BaTiO_3 and $(001)_p$ SrTiO_3 layers, respectively. Despite the 2.3% lattice mismatch between the $(001)_p$ BaTiO_3 and $(001)_p$ SrTiO_3 layers, such superlattices can be commensurately strained. In **Figure 3**, the structural characterization of a commensurate $(\text{BaTiO}_3)_n/(\text{SrTiO}_3)_m$ superlattice with $n = 1$ and $m = 30$ is shown. The macroscopic regularity of this superlattice, which was grown by molecular beam epitaxy (MBE), is demonstrated by the presence and sharpness of all of the superlattice reflections in its x-ray diffraction pattern (see Figure 3b).^{60,119} Despite the BaTiO_3 layer being just a single unit cell thick (0.4 nm) and well-separated from neighboring BaTiO_3 layers, ultraviolet Raman measurements show that it is still ferroelectric.⁶⁰

The ability to compare theory and experiment has motivated refinements in theory, including attention to not only mechanical (strain) and electrical boundary conditions (whether the ferroelectric is bounded by conducting electrodes or insulating layers), but also to unequal biaxial strain^{115,116} and the ability of a ferroelectric film to break up into multiple domains.^{97,98} For strained-layer superlattices of $\text{BaTiO}_3/\text{SrTiO}_3$, it was shown that quantitative agreement between the predicted and observed T_C for superlattices with a wide range of periodicities only occurred if calculations in which the possibility of multiple domains was considered.^{109,110} For some $\text{BaTiO}_3/\text{SrTiO}_3$ superlattices, such three-dimensional phase-field calculations indicated that the low energy configuration was a multiple-domain state, which allowed the polarization in the $(001)_p$ SrTiO_3 layers to drop considerably when the $(001)_p$ BaTiO_3 layer was thinner than the $(001)_p$ SrTiO_3 layer, resulting in a significant increase in T_C compared to the single-domain state.^{109,110} The domains anticipated to be present by theory, in order to quantitatively explain the observed T_C values, have recently been observed in $\text{BaTiO}_3/\text{SrTiO}_3$ strained-layer superlattices.^{117,118}

Strain engineering of multiferroics

Emboldened by these successes, the strain game has more recently turned to enhancing materials containing multiple ferroic order parameters (i.e., multiferroics such as BiFeO_3) or to create new multiferroics from materials that are on the verge of being ferroic (e.g., EuTiO_3). Illustrative examples are described in the sections that follow.

Strained BiFeO_3 —Morphing a room-temperature multiferroic

Bismuth ferrite, BiFeO_3 , is one of the few materials that is simultaneously ferroelectric and magnetically ordered (antiferromagnetically in the case of BiFeO_3) at room temperature.^{120–124} All of the other room-temperature multiferroics are, however, metastable. These include the high-pressure phase BiCoO_3 ,¹²² strain-stabilized ScFeO_3 with the corundum structure,¹²³ and the hexagonal polymorph of LuFeO_3 that has been stabilized via epitaxy.¹²⁴ In its unstrained state, BiFeO_3 has the highest remnant polarization of any known ferroelectric.^{120,121,125–127} BiFeO_3 also exhibits several polymorphs that are relatively close in energy to each other. Further, in BiFeO_3 , the four fundamental degrees of freedom—electronic

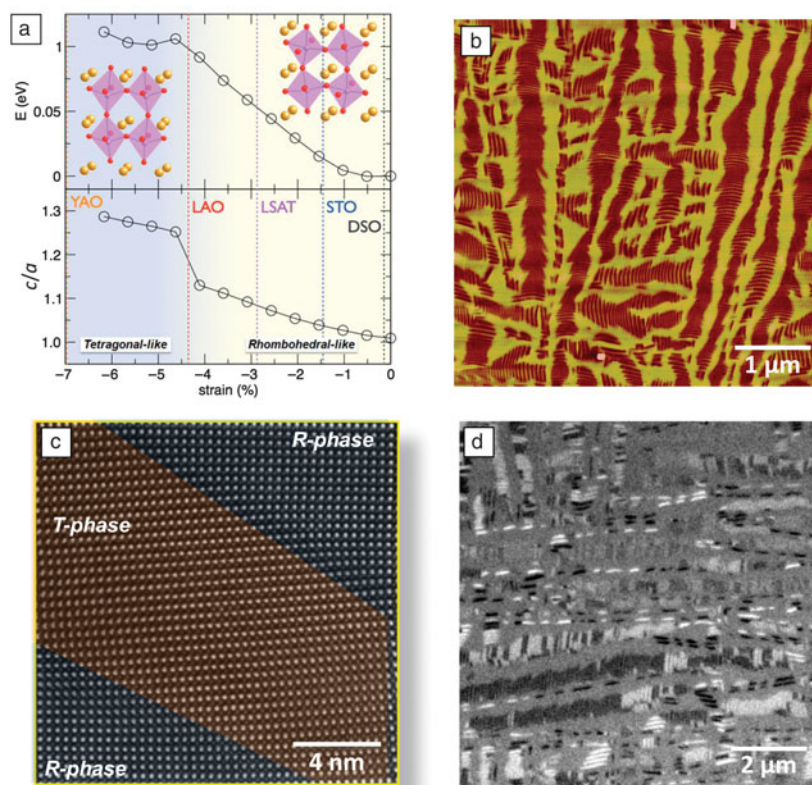


Figure 4. (a) *Ab initio* calculations of the energy and structure (ratio of pseudotetragonal lattice constants c/a) of the ground state of BiFeO_3 as a function of bi-axial, in-plane compressive strain on various substrates: YAO, YAlO_3 ; LAO, LaAlO_3 ; STO, SrTiO_3 ; LSAT, $(\text{LaAlO}_3)_{0.29}-(\text{SrAl}_{1/2}\text{Ta}_{1/2}\text{O}_3)_{0.71}$; DSO, DyScO_3 . (b) Atomic force microscopy image of a partially relaxed, ~ 70 -nm-thick BiFeO_3 film grown on a LaAlO_3 substrate that exhibits a characteristic tetragonal and rhombohedral (T+R) mixed phase nanostructure. (c) High-resolution transmission electron microscopy image of the T+R mixed phase that illustrates the commensurate nature of the interface, with the complete absence of misfit dislocations. (d) X-ray magnetic circular dichroism photoemission electron microscopy (XMCD-PEEM) image obtained using the iron absorption edge showing that the highly constrained R-phase shows enhanced ferromagnetism compared to the bulk or the T-phase. Enhanced magnetic contrast is given from the ratio of PEEM images taken with left and right circularly polarized x-rays at the same location. Black and white contrasts indicate magnetic moments pointing parallel and antiparallel to the incident x-rays. (a) Reprinted with permission from Reference 21. © 2009 AAAS. (b) Adapted from Reference 21. (c) Reprinted with permission from Reference 21. © 2009 AAAS. (d) Reprinted with permission from Reference 134. © 2011 Nature Publishing Group.

spin, charge, orbital, and lattice—are highly interactive. As a consequence, its ground state exhibits a strong sensitivity to temperature, pressure, electric fields, and magnetic fields. These qualities make BiFeO₃ unique and a natural candidate to tweak using the strain game.

Elastic strain, imparted via epitaxy, is able to distort and eventually change the structure and energy of the ground state of BiFeO₃. In its unstrained state, BiFeO₃ is rhombohedral.¹²⁸ The evolution of the structure of BiFeO₃ can be understood from *ab initio* calculations, **Figure 4a**. As an in-plane biaxial compressive strain is imposed via the substrate, the rhombohedral (R) structure becomes progressively monoclinic (and perhaps even triclinic) until a critical strain of ~4.5% is reached. For substrates that impose a larger strain (such as (110) YAlO₃, which imposes a hefty 6.6% biaxial compressive strain on commensurate BiFeO₃ thin films grown upon it^{21–24}), the structure changes into a “super-tetragonal” (T) state (or a monoclinic derivative thereof) with a distinct jump in the ratio of its pseudotetragonal lattice constants *c/a*.²¹ Such an isostructural monoclinic-to-monoclinic phase transition—in which the symmetry does not change, but the coordination chemistry changes dramatically—has also been observed in other materials.^{129–132} The overlapping, roughly parabolic free energy versus strain curves of the R- and T-phases can be seen in **Figure 4a**. It is the change in ground state with strain from the R phase to the T phase that enables the huge (6.6%) biaxial strains to be achieved in BiFeO₃ films. In more typical oxide systems, the free energy versus strain landscape limits the growth of epitaxial perovskite films under common growth conditions to about 3% strain.

Partial relaxation of the epitaxial constraint by increasing the film thickness leads to the formation of a mixed-phase nanostructure that exhibits the coexistence of both the R- and T-phases, as illustrated in the atomic force microscope (AFM) image in **Figure 4b**. This mixed-phase nanostructure is fascinating from many perspectives. First, high-resolution electron microscopy shows that the interface between these two phases is essentially commensurate, **Figure 4c**. This is important because it means that movement of this interface should be possible simply by the application of an electric field, as is indeed the case.¹³³ Second, and perhaps more importantly, the highly distorted R-phase in this ensemble, shows significantly enhanced ferromagnetism. This can be discerned from the x-ray magnetic circular dichroism-photoemission electron microscopy (XMCD-PEEM) image in **Figure 4d**. The R-phase appears in either bright or dark stripe-like contrast in such PEEM images, corresponding to the thin slivers being magnetized either along the x-ray polarization direction or anti-parallel to it.

A rough estimate of the magnetic moment of this highly strained R-phase (from the PEEM images as well as from superconducting quantum interference device magnetometry measurements) gives a local moment of the order of 25–35 emu/cc.¹³⁴ It is noteworthy that the canted moment of the R-phase (~6–8 emu/cc) is not observable by the XMCD technique due to the small magnitude of the moment. This enhanced magnetic moment in the highly strained R-phase

disappears around 150°C.¹³⁴ Application of an electric field converts this mixed (R+T) phase into the T-phase, and the enhanced magnetic moment disappears; reversal of the electric field brings the mixed phase back accompanied by the magnetic moment in the distorted R-phase.¹³⁴

There has been limited work on the tensile side of the BiFeO₃ strain phase diagram. It was, however, predicted, using phase-field calculations, that an orthorhombic (O) phase of BiFeO₃ should exist under sufficient tensile strain,²¹ and recent work has shown that an O-phase can indeed be stabilized.¹³⁵ These observations on biaxially strained BiFeO₃ films raise several questions. First, what is the magnetic ground state of the various strained BiFeO₃ phases (e.g., do they have enhanced canting or exhibit spin glass behavior?). Second, given that spin-orbit coupling is the source of the canted moment in the bulk of BiFeO₃, can this enhanced moment be explained based on the strain and confinement imposed on the R-phase? Finally, what is the state of the Dzyaloshinskii–Moriya vector, the antisymmetric microscopic coupling between two localized magnetic moments, in such a strained system?

Strained EuTiO₃—Transforming a boring dielectric into the world's strongest ferroelectric ferromagnet

The strain game involving EuTiO₃ is another tale in which theory led the way to a remarkable strain-enabled discovery. The idea behind this new route to ferroelectric ferromagnets is that appropriate magnetically ordered insulators that are neither ferroelectric nor ferromagnetic, of which there are many, can be transmuted into ferroelectric ferromagnets. Fennie and Rabe predicted¹³⁶ that EuTiO₃, a normally boring paraelectric and antiferromagnetic insulator (in its unstrained bulk state), could be transformed using strain into the strongest known multiferroic with a spontaneous polarization and spontaneous magnetization each 100× superior to the reigning multiferroic it displaced, Ni₃B₇O₁₃I.^{137,138}

The physics behind this discovery makes use of spin-lattice coupling as an additional parameter to influence the soft mode of an insulator on the verge of a ferroelectric transition.¹³⁹ The soft mode is the lowest frequency transverse optical phonon, which as it goes to zero results in the phase transition from a paraelectric to a ferroelectric. Appropriate materials for this (1) have a ground state that in the absence of strain is antiferromagnetic and paraelectric, (2) are on the brink of a ferroelectric transition, and (3) exhibit large spin-lattice coupling manifested by a significant decrease in permittivity as the material is cooled through its Néel temperature.¹³⁶ EuTiO₃ meets these criteria and has much in common with SrTiO₃ except that EuTiO₃ magnetically orders at 5 K due to the existence of localized 4*f* moments on the Eu²⁺ site.^{140,141} Similar to SrTiO₃, strain can be used to soften the soft mode and drive it to a ferroelectric instability. In contrast to SrTiO₃, which is diamagnetic, the permittivity of bulk EuTiO₃ is strongly coupled with its magnetism, showing an abrupt decrease in permittivity at the onset of the antiferromagnetic Eu²⁺ ordering.¹⁴² This indicates that the

soft mode frequency hardens when the spins order antiferromagnetically; conversely, it will soften if the spins order ferromagnetically. This extra interaction provides the coupling favoring a simultaneously ferroelectric and ferromagnetic ground state under sufficient strain in EuTiO_3 .

Although testing this prediction seems straightforward, the groups who first tested it ran into an unforeseen complication: no matter what substrate they deposited EuTiO_3 on, it was ferromagnetic. With its identical lattice constant (both are 3.905 Å at room temperature), SrTiO_3 is an obvious substrate for the growth of unstrained epitaxial EuTiO_3 films. Surprisingly, as-grown $\text{EuTiO}_{3-\delta}$ thin films synthesized by pulsed-laser deposition (PLD) on (001) SrTiO_3 substrates exhibit expanded out-of-plane spacings (0.4% to 2% longer than bulk EuTiO_3)^{143–146} and are ferromagnetic with a Curie temperature of about 5 K.^{144,145}

Could the observed expanded lattice spacings in $\text{EuTiO}_{3-\delta}$ thin films be due to oxygen vacancies? The effect of oxygen deficiency on lattice constant has been studied in $\text{EuTiO}_{3-\delta}$ bulk samples down to the $\text{EuTiO}_{2.5}$ limit of the perovskite $\text{EuTiO}_{3-\delta}$ structure, and negligible (<0.5%) variation in the cubic lattice constant was found.^{147,148} Oxygen vacancies alone are thus insufficient to explain the 2% variation in out-of-plane lattice spacings observed in epitaxial $\text{EuTiO}_{3-\delta}$ films grown on (001) SrTiO_3 by PLD.^{144–146}

One possible explanation is that the ferromagnetism observed in epitaxial EuTiO_3 films prepared by PLD on SrTiO_3 arises from extrinsic effects, masking the intrinsic properties of EuTiO_3 thin films. Extrinsic effects are known to occur in thin films, particularly for deposition methods involving energetic species, which can induce defects. Another factor favoring defect introduction is the relatively low growth temperatures common for oxide thin-film growth, enabling defects to be frozen in. For example, some epitaxial SrTiO_3 films grown on SrTiO_3 substrates by PLD have been reported to be ferroelectric,¹⁴⁹ in striking contrast to the intrinsic nature of unstrained SrTiO_3 , which is not ferroelectric at any temperature.¹⁵⁰ Homoepitaxial SrTiO_3 films grown by PLD are also known to exhibit lattice spacings that deviate significantly from the SrTiO_3 substrates they are grown on,^{151–153} although bulk $\text{SrTiO}_{3-\delta}$ (in either single crystal or polycrystalline form) exhibits negligible variation in its cubic lattice constant up to the $\text{SrTiO}_{2.5}$ limit^{154,155} of the perovskite $\text{SrTiO}_{3-\delta}$ structure. The sensitivity of EuTiO_3 that made it an appropriate material to transmute via strain into a multiferroic also makes it quite sensitive to defects.

To overcome this issue and examine the intrinsic effect of strain on EuTiO_3 , a more delicate deposition technique was needed.

In contrast to PLD, homoepitaxial SrTiO_3 films grown by MBE¹⁵⁶ show bulk behavior and none of the unusual effects reported in homoepitaxial SrTiO_3 films grown by PLD.^{149,151–153} Indeed unstrained, stoichiometric EuTiO_3 thin films grown by MBE on (001) SrTiO_3 have the same lattice constant as bulk EuTiO_3 and are antiferromagnetic.¹⁵⁷ Seeing that MBE can produce EuTiO_3 films with intrinsic properties in their unstrained state, MBE was used to test Fennie and Rabe's strained EuTiO_3 predictions.¹³⁶ Commensurate EuTiO_3 films were grown on three substrates: (001) LSAT, (001) SrTiO_3 , and (110) DyScO_3 to impart -0.9% , 0% , and $+1.1\%$ biaxial

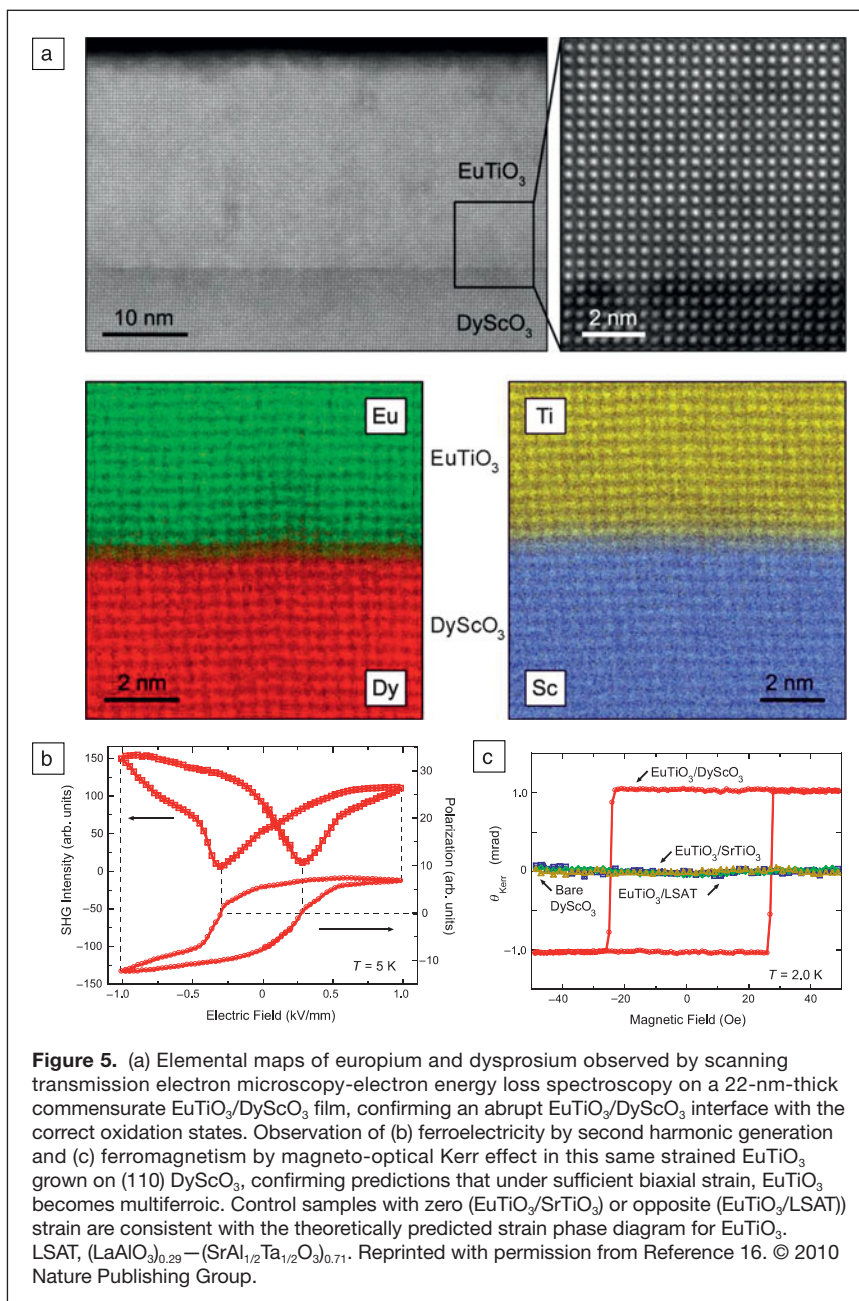


Figure 5. (a) Elemental maps of europium and dysprosium observed by scanning transmission electron microscopy-electron energy loss spectroscopy on a 22-nm-thick commensurate $\text{EuTiO}_3/\text{DyScO}_3$ film, confirming an abrupt $\text{EuTiO}_3/\text{DyScO}_3$ interface with the correct oxidation states. Observation of (b) ferroelectricity by second harmonic generation and (c) ferromagnetism by magneto-optical Kerr effect in this same strained EuTiO_3 grown on (110) DyScO_3 , confirming predictions that under sufficient biaxial strain, EuTiO_3 becomes multiferroic. Control samples with zero ($\text{EuTiO}_3/\text{SrTiO}_3$) or opposite ($\text{EuTiO}_3/\text{LSAT}$) strain are consistent with the theoretically predicted strain phase diagram for EuTiO_3 . LSAT, $(\text{LaAlO}_3)_{0.29}-(\text{SrAl}_{1/2}\text{Ta}_{1/2}\text{O}_3)_{0.71}$. Reprinted with permission from Reference 16. © 2010 Nature Publishing Group.

strain, respectively. Using scanning transmission electron microscopy with electron energy loss spectroscopy (STEM-EELS), the oxidation state of the film constituents and the abruptness of the interface between the film and substrate was checked with atomic resolution and chemical specificity (**Figure 5a**). Experimental measurements utilizing second harmonic generation (SHG) and magneto-optic Kerr effect (MOKE) confirmed that the EuTiO_3 grown on (110) DyScO_3 was simultaneously ferroelectric (**Figure 5b**) and ferromagnetic (**Figure 5c**), while on the other substrates it was not, in agreement with theory¹³⁶ and resulting in the strongest multiferroic material known today.¹⁶

There are many other exciting predictions that remain to be verified of even stronger and higher temperature ferroelectric ferromagnets in strained SrMnO_3 ¹⁵⁸ and EuO ,¹⁵⁹ as well as the prediction that an electric field on the order of 10^5 V cm^{-1} can be used to turn on ferromagnetism in EuTiO_3 when it is poised on the verge of such a phase transition via strain.¹³⁶ It was recently shown that through the application of an electric field, the antiferromagnetic ground state of EuTiO_3 , strained to be close to where it would have a ferromagnetic ground state (but still on the antiferromagnetic side), can be electrically tuned to the verge of the ferromagnetic state.¹⁶⁰ Turning on magnetism in a material by applying an electric field to it remains an open challenge. Such an important milestone would be a key advance to the field of ferroics, both scientifically and technologically.

Electronics has flourished because of the ability to route voltages with ease and on extremely small scales. If magnetism could be similarly controlled and routed, it would impact memory devices, spin valves, and many other spintronics devices and make numerous hybrid devices possible.

Strained $\text{Sr}_{n+1}\text{Ti}_n\text{O}_{3n+1}$ —Creating a tunable dielectric with record performance

Strain has also been used to create a new family of tunable microwave dielectrics, which due to their low dielectric loss have a figure of merit at room temperature that rivals those of all such known materials.¹⁶¹ In contrast to standard (textbook) dielectrics, whose dielectric displacement (**D**) as a function of applied electric field (**E**) can be described by the linear equation

$$\mathbf{D} = \epsilon_0 \mathbf{K} \mathbf{E}, \quad (1)$$

where ϵ_0 is the permittivity of free space and **K** is the dielectric constant of the material, a tunable dielectric has a highly nonlinear relationship between **D** and **E**. The nonlinearity results in the effective dielectric constant of the material ($\mathbf{D}/\epsilon_0\mathbf{E}$) behaving not as a constant, but changing greatly with **E**; changes of tens of percent in the dielectric “constant” are common in tunable dielectrics at high **E**. This nonlinearity can be described by adding higher order terms to Equation 1. In tensor form, this more general relationship is

$$D_i = \epsilon_0 K_{ij} E_j + \epsilon_{ijk} E_j E_k + \epsilon_{ijkl} E_j E_k E_l + \dots, \quad (2)$$

where ϵ_{ijk} and ϵ_{ijkl} are higher order permittivity coefficients.

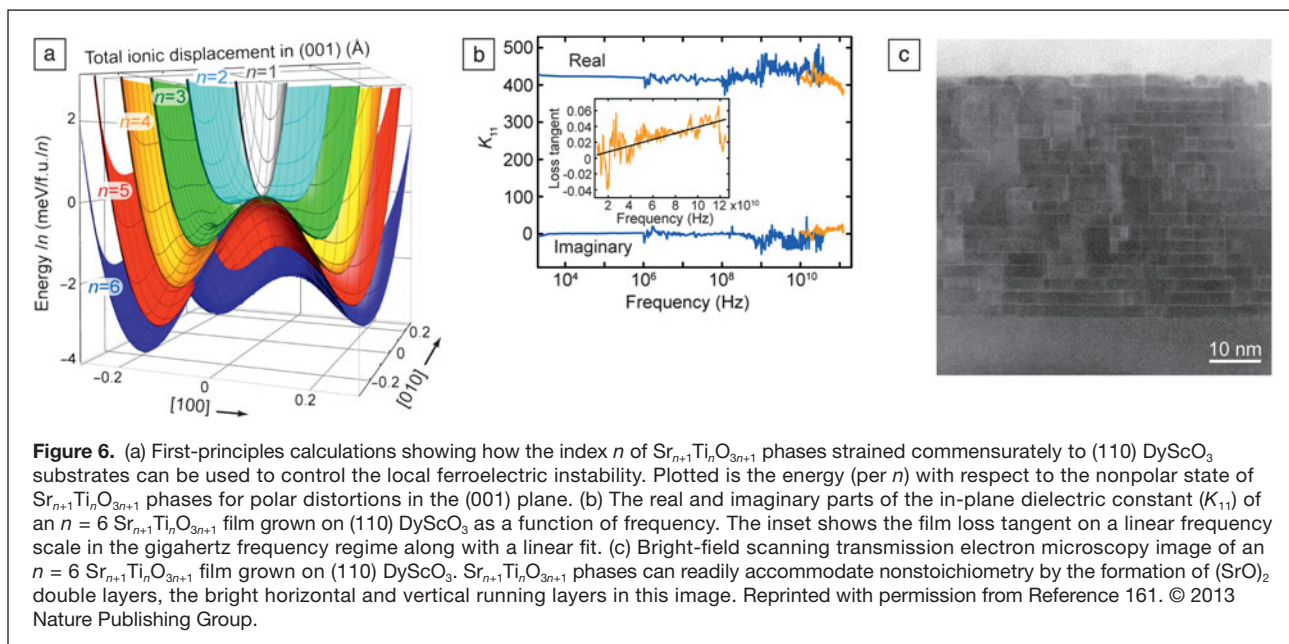
Highly nonlinear dielectrics, including the most extensively studied material with such properties, $\text{Ba}_x\text{Sr}_{1-x}\text{TiO}_3$,^{162–165} are found in displacive ferroelectric systems at temperatures just above the paraelectric-to-ferroelectric transition temperature.^{162,165} These tunable dielectrics are normally used in their paraelectric state to avoid the dielectric losses that would occur in the ferroelectric state due to the motion of domain walls. Although thin films provide an excellent geometry for the application of high **E** at low applied voltages, $\text{Ba}_x\text{Sr}_{1-x}\text{TiO}_3$ films unfortunately suffer significant dielectric losses arising from defects; the dielectric loss in today’s best $\text{Ba}_x\text{Sr}_{1-x}\text{TiO}_3$ tunable dielectrics films at GHz frequencies is about an order of magnitude worse than the best $\text{Ba}_x\text{Sr}_{1-x}\text{TiO}_3$ in bulk form.¹⁶⁵

A new approach to tunable microwave dielectrics is to take a system with exceptionally low loss and introduce a ferroelectric instability into it using strain. The appeal of this approach is that it can be applied to systems that are known to have exceptionally low dielectric loss, particularly in thin-film form. Such systems do not need to have a ferroelectric instability in their unstrained form; strain can be used to help impart the ferroelectric instability. This relaxed design constraint greatly increases the number of eligible systems that could yield improved performance over the best of today’s known tunable dielectrics.

This approach has been applied to $\text{Sr}_{n+1}\text{Ti}_n\text{O}_{3n+1}$ phases—where $(\text{SrO})_2$ crystallographic shear^{166,167} planes provide an alternative to point-defect formation for accommodating nonstoichiometry.^{168,169} These phases are known to have low dielectric loss,^{170,171} even in thin-film form.¹⁷² In their unstrained state, these phases are centrosymmetric, and thus lack a ferroelectric instability.

The strain game in combination with control of the distance between the $(\text{SrO})_2$ planes in $\text{Sr}_{n+1}\text{Ti}_n\text{O}_{3n+1}$ phases can, however, induce a ferroelectric instability.^{161,173} The emergence of this ferroelectric instability in $\text{Sr}_{n+1}\text{Ti}_n\text{O}_{3n+1}$ phases commensurately strained in biaxial tension to (110) DyScO_3 substrates (about 1% biaxial tension) can be seen in **Figure 6a**. For $n \geq 3$, a ferroelectric instability is evident from the double-well energy potential of the ion displacements, and this double-well becomes deeper with increasing n . A deeper well corresponds to the ferroelectric instability occurring at higher temperature until, by $n = 6$, it is just below room temperature.¹⁶¹

The low loss of this tunable dielectric at high frequencies is evident from **Figure 6b**, where both the real and imaginary parts of the in-plane dielectric constant K_{11} are shown over a frequency range spanning more than eight orders of magnitude and up to 125 GHz.¹⁶¹ Only at these highest frequencies can the dielectric loss be seen. This low loss yields unparalleled performance at room temperature for these new tunable dielectrics.¹⁶⁴ The reason for the low dielectric loss, far lower than today’s best $\text{Ba}_x\text{Sr}_{1-x}\text{TiO}_3$ tunable dielectrics at GHz frequencies, is believed to be related to the propensity of $\text{Sr}_{n+1}\text{Ti}_n\text{O}_{3n+1}$ phases to form $(\text{SrO})_2$ planar defects in response to



local stoichiometry deviations rather than point defects.^{168,169} These $(\text{SrO})_2$ double layers show up as bright layers in the STEM image of an $n = 6$ $\text{Sr}_{n+1}\text{Ti}_n\text{O}_{3n+1}$ film in Figure 6c. This is in contrast to the high point-defect concentrations that perovskite films like SrTiO_3 can incorporate in thin-film form,^{75,156} such point defects could be the reason that $\text{Ba}_x\text{Sr}_{1-x}\text{TiO}_3$ tunable dielectric films have significantly higher dielectric losses than bulk $\text{Ba}_x\text{Sr}_{1-x}\text{TiO}_3$.¹⁶⁵

Other ways oxides can react to strain

As the examples described in this article show, the strain game can be a powerful control parameter for enhancing the properties of ferroic oxides. It is important to consider, however, other ways in which a complex oxide might react to strain. Should there be an energetically more favorable route to accommodate the imposed strain, the system might take it. Examples include the possibility that the imposed strain will lead to changes in film composition, microstructure, or crystal structure (e.g., ordering [or disordering] of cations, anions, or their vacancies,^{174,175} atom clustering, the stabilization of other polymorphs, or rotations of the oxygen coordination polyhedra^{176–178}) rather than simply dilating or compressing the spacings between the atoms in the unstrained structure equally. Octahedral rotation patterns from underlying layers and substrates can be imparted into films over distances of several nanometers and can thus complicate a simple biaxial strain picture. An example is the creation of T-phase BiFeO_3 at relatively low biaxial strain (-1.4% , where the BiFeO_3 should be monoclinic), due to the competition between different octahedral rotation patterns in the film and in the substrate.¹⁷⁹ Such chemical and structural changes may also cause dramatic changes in properties, for better or worse, but it is important to distinguish the underlying causes of the changes in properties.

Advances in electron microscopy have been particularly beneficial in identifying these underlying causes (see the Hÿtch and Minor article in this issue). With respect to ferroics, recent advances enabling polarization mapping on the atomic scale,^{180–183} octahedral rotation imaging,¹⁸⁴ and improved STEM-EELS analysis¹⁸⁵ are invaluable in separating true strain effects from changes in composition, structure, and microstructure that can occur to mitigate against a strain effect. These techniques have the potential to visualize closure domains in ferroelectrics,^{182,183} usual domain walls with mixed Bloch–Néel–Ising character in strained ferroelectric superlattices,¹⁸⁶ and the exciting possibility of a dipole-dipole coupling analog of exchange-spring magnets^{187,188} recently predicted to occur in strained ferroelectric systems.¹⁸⁹

Other intriguing predictions, including using strain to poise a material (e.g., SrCoO_3 ¹⁹⁰) on the brink of a metal-insulator transition, which could then be turned on or off through the application of an electric or magnetic field or even a small additional strain, are relevant to emerging piezotronic devices.^{191,192}

Outlook

Elastic strain engineering of ferroics with the perovskite structure has been the most pursued to date. Yet there are many other fascinating oxides that either have a ferroic ground state or are borderline ferroic materials that might be enticed into a ferroic ground state with strain. Such non-perovskite structural families that are relevant include chrysoberyl Cr_2BeO_4 ,¹⁹³ pyrochlore $\text{Ho}_2\text{Ti}_2\text{O}_7$,¹⁹⁴ YMnO_3 ,^{195,196} MnWO_4 ,¹⁹⁷ delafossite CuFeO_2 ,¹⁹⁸ CuO ,¹⁹⁹ and hexaferrite $\text{Sr}_3\text{Co}_2\text{Fe}_{24}\text{O}_{41}$.²⁰⁰ These systems are generally ignored by the thin-film community and have been the focus of the single crystal ferroic community. We believe the issue is the lack of suitable substrates for these latter structures; removing this roadblock would unleash a

huge opportunity in strain engineering for the future. Thin films also have the technological advantage of lower switching voltages and the ability to integrate them into more sophisticated heterostructures, as are relevant for devices.

Imagine the opportunities for strain engineering that substrates for the non-perovskite systems would bring. Substrates for YMnO_3 would enable more variants of hexagonal manganese ferroics to be constructed. These variants include not only known materials, but metastable polymorphs (e.g., LuFeO_3 that is isostructural to YMnO_3 rather than its stable centrosymmetric perovskite form)^{124,201,202} by utilizing lattice misfit strain energies and interfacial energies to favor the desired metastable phase over the equilibrium phase (epitaxial stabilization),^{203–206} or the prospect of interfacial multiferroicity that has been predicted to emerge in superlattices between centrosymmetric components.^{207,208}

Similarly, substrates with the LiNbO_3 structure would enable the growth of the LiNbO_3 -polymorph of FeTiO_3 and related multiferroics.^{209,210} A range of appropriate substrates, like the range of substrates available for perovskites shown in Figure 1d, for each ferroic system of interest would allow the thin-film tricks of strain engineering,^{12–16} epitaxial stabilization,^{203–206} dimensional confinement,^{161,173} polarization engineering,^{112,211} and superlattice formation^{60,103–114,117–119,207,208} to be freely applied to a much larger set of ferroic building blocks. Strain engineering of ferroic oxides is in its infancy and considering its brief, but vibrant past, a brilliant future awaits.

Acknowledgments

We gratefully acknowledge our colleagues and collaborators for sharing their insights and helping us to explore and better understand the exciting area of elastically strained ferroic oxide films. We especially thank the groups of E. Arenholz, M. Bedzyk, M.D. Biegalski, D.H.A. Blank, D.A. Bonnell, J.C. Booth, J.D. Brock, L.E. Cross, C.B. Eom, J.W. Freeland, P. Ghosez, P.C. Hammel, M.E. Hawley, E. Johnston-Halperin, S. Kamba, S.W. Kirchoefer, J. Levy, Yulan Li, T.E. Mallouk, J. Mannhart, L.W. Martin, K. Peters, K.M. Rabe, J.M. Rondinelli, P.J. Ryan, P. Schiffer, J. Schubert, N.A. Spaldin, S.K. Streiffer, A.K. Tagantsev, I. Takeuchi, D.A. Tenne, J.-M. Triscone, S. Trolier-McKinstry, D. Vanderbilt, J.C. Woicik, and X.X. Xi. L.Q.C., C.J.F., V.G., X.Q.P., D.G.S., and R.R. gratefully acknowledge financial support from the National Science Foundation (NSF) under Grant No. DMR-0820404. D.G.S. also acknowledges NSF Grant DMR-0948036. R.R. acknowledges sustained support from the US Department of Energy under Contract No. DE-AC0205CH11231.

References

1. A.E. Lindh, in *Nobel Lectures in Physics 1942–1962* (World Scientific, Singapore, 1998), pp. 49–52.
2. J.M. Lock, *Philos. Trans. R. Soc. London, Ser. A* **208**, 391 (1951).
3. P.W. Forsbergh Jr., *Phys. Rev.* **93**, 686 (1954).
4. L.D. Nguyen, A.S. Brown, M.A. Thompson, L.M. Jelloian, *IEEE Trans. Electron Devices* **39**, 2007 (1992).
5. J. Welser, J.L. Hoyt, J.F. Gibbons, *IEEE Electron Device Lett.* **15**, 100 (1994).
6. W. Shockley, J. Bardeen, *Phys. Rev.* **77**, 407 (1950).

7. H. Sato, M. Naito, *Physica C* **274**, 221 (1997).
8. I. Bozovic, G. Logvenov, I. Belca, B. Narimbetov, I. Sveklo, *Phys. Rev. Lett.* **89**, 107001 (2002).
9. R.S. Beach, J.A. Borchers, A. Matheny, R.W. Erwin, M.B. Salamon, B. Everitt, K. Pettit, J.J. Rhyne, C.P. Flynn, *Phys. Rev. Lett.* **70**, 3502 (1993).
10. Q. Gan, R.A. Rao, C.B. Eom, J.L. Garrett, M. Lee, *Appl. Phys. Lett.* **72**, 978 (1998).
11. D. Fuchs, E. Arac, C. Pinta, S. Schuppler, R. Schneider, H.v. Löhneysen, *Phys. Rev. B* **77**, 014434 (2008).
12. J.H. Haeni, P. Irvin, W. Chang, R. Uecker, P. Reiche, Y.L. Li, S. Choudhury, W. Tian, M.E. Hawley, B. Craigo, A.K. Tagantsev, X.Q. Pan, S.K. Streiffer, L.Q. Chen, S.W. Kirchoefer, J. Levy, D.G. Schlom, *Nature* **430**, 758 (2004).
13. K.J. Choi, M.D. Biegalski, Y.L. Li, A. Sharan, J. Schubert, R. Uecker, P. Reiche, Y.B. Chen, X.Q. Pan, V. Gopalan, L.-Q. Chen, D.G. Schlom, C.B. Eom, *Science* **306**, 1005 (2004).
14. D.G. Schlom, L.Q. Chen, C.B. Eom, K.M. Rabe, S.K. Streiffer, J.-M. Triscone, *Annu. Rev. Mater. Res.* **37**, 589 (2007).
15. M.P. Warusawithana, C. Cen, C.R. Slesman, J.C. Woicik, Y.L. Li, L.F. Kourkoutis, J.A. Klug, H. Li, P. Ryan, L.-P. Wang, M. Bedzyk, D.A. Muller, L.Q. Chen, J. Levy, D.G. Schlom, *Science* **324**, 367 (2009).
16. J.H. Lee, L. Fang, E. Vlahos, X. Ke, Y.W. Jung, L.F. Kourkoutis, J.-W. Kim, P.J. Ryan, T. Heeg, M. Roeckerath, V. Goian, M. Bernhagen, R. Uecker, P.C. Hammel, K.M. Rabe, S. Kamba, J. Schubert, J.W. Freeland, D.A. Muller, C.J. Fennie, P. Schiffer, V. Gopalan, E. Johnston-Halperin, D.G. Schlom, *Nature* **466**, 954 (2010).
17. C. Adamo, X. Ke, H.Q. Wang, H.L. Xin, T. Heeg, M.E. Hawley, W. Zander, J. Schubert, P. Schiffer, D.A. Muller, L. Maritato, D.G. Schlom, *Appl. Phys. Lett.* **95**, 112504 (2009).
18. H. Béa, B. Dupé, S. Fusil, R. Mattana, E. Jacquet, B. Warot-Fonrose, F. Wilhelm, A. Rogalev, S. Petit, V. Cros, A. Anane, F. Petroff, K. Bouzehouane, G. Geneste, B. Dkhil, S. Lisenkov, I. Ponomareva, L. Bellaiche, M. Bibes, A. Barthélémy, *Phys. Rev. Lett.* **102**, 217603 (2009).
19. I.C. Infante, S. Lisenkov, B. Dupé, M. Bibes, S. Fusil, E. Jacquet, G. Geneste, S. Petit, A. Courtial, J. Juraszek, L. Bellaiche, A. Barthélémy, B. Dkhil, *Phys. Rev. Lett.* **105**, 057601 (2010).
20. Z. Chen, Z. Luo, C. Huang, Y. Qi, P. Yang, L. You, C. Hu, T. Wu, J. Wang, C. Gao, T. Sritharan, L. Chen, *Adv. Funct. Mater.* **21**, 133 (2011).
21. R.J. Zeches, M.D. Rossell, J.X. Zhang, A.J. Hatt, Q. He, C.-H. Yang, A. Kumar, C.H. Wang, A. Melville, C. Adamo, G. Sheng, Y.-H. Chu, J.F. Ihlefeld, R. Erni, C. Ederer, V. Gopalan, L.Q. Chen, D.G. Schlom, N.A. Spaldin, L.W. Martin, R. Ramesh, *Science* **326**, 977 (2009).
22. P. Chen, N.J. Podraza, X.S. Xu, A. Melville, E. Vlahos, V. Gopalan, R. Ramesh, D.G. Schlom, J.L. Musfeldt, *Appl. Phys. Lett.* **96**, 131907 (2010).
23. H.M. Christen, J.H. Nam, H.S. Kim, A.J. Hatt, N.A. Spaldin, *Phys. Rev. B* **83**, 144107 (2011).
24. L.W. Martin, D.G. Schlom, *Curr. Opin. Solid State Mater. Sci.* **16**, 199 (2012).
25. A.A. Griffith, *Philos. Trans. R. Soc. London, Ser. A* **221**, 163 (1920).
26. E. Klokholm, J.W. Matthews, A.F. Mayadas, J. Angiello, in *Magnetism and Magnetic Materials*, C.D. Graham Jr., J.J. Rhyne, Eds. (American Institute of Physics, New York, 1972), pp. 105–109.
27. L.B. Freund, S. Suresh, *Thin Film Materials: Stress, Defect Formation and Surface Evolution* (Cambridge University Press, Cambridge, 2003), pp. 60–83, 283–290, 396–416.
28. N.A. Pertsev, A.K. Tagantsev, N. Setter, *Phys. Rev. B* **61**, R825 (2000).
29. N.A. Pertsev, A.K. Tagantsev, N. Setter, *Phys. Rev. B* **65**, 219901 (2002).
30. A.F. Devonshire, *Philos. Mag.* **3** (Suppl.), 85 (1954).
31. A. Antons, J.B. Neaton, K.M. Rabe, D. Vanderbilt, *Phys. Rev. B* **71**, 024102 (2005).
32. Y.L. Li, S. Choudhury, J.H. Haeni, M.D. Biegalski, A. Vasudevarao, A. Sharan, H.Z. Ma, J. Levy, V. Gopalan, S. Trolier-McKinstry, D.G. Schlom, Q.X. Jia, L.Q. Chen, *Phys. Rev. B* **73**, 184112 (2006).
33. C.L. Canedy, H. Li, S.P. Alpay, L. Salamanca-Riba, A.L. Roytburd, R. Ramesh, *Appl. Phys. Lett.* **77**, 1695 (2000).
34. I.B. Misirlioglu, A.L. Vasiliev, M. Aindow, S.P. Alpay, R. Ramesh, *Appl. Phys. Lett.* **84**, 1742 (2004).
35. M.-W. Chu, I. Szafrański, R. Scholz, C. Harnagea, D. Hesse, M. Alexe, U. Gösele, *Nature Mater.* **3**, 87 (2004).
36. S.P. Alpay, I.B. Misirlioglu, V. Nagarajan, R. Ramesh, *Appl. Phys. Lett.* **85**, 2044 (2004).
37. V. Nagarajan, C.L. Jia, H. Kohlstedt, R. Waser, I.B. Misirlioglu, S.P. Alpay, R. Ramesh, *Appl. Phys. Lett.* **86**, 192910 (2005).
38. M.D. Biegalski, D.D. Fong, J.A. Eastman, P.H. Fuoss, S.K. Streiffer, T. Heeg, J. Schubert, W. Tian, C.T. Nelson, X.Q. Pan, M.E. Hawley, M. Bernhagen, P. Reiche, R. Uecker, S. Trolier-McKinstry, D.G. Schlom, *J. Appl. Phys.* **104**, 114109 (2008).
39. R. Uecker, H. Wilke, D.G. Schlom, B. Velickov, P. Reiche, A. Polity, M. Bernhagen, M. Rossberg, *J. Cryst. Growth* **295**, 84 (2006).

40. R. Uecker, B. Velickov, D. Klimm, R. Bertram, M. Bernhagen, M. Rabe, M. Albrecht, R. Fornari, D.G. Schlom, *J. Cryst. Growth* **310**, 2649 (2008).
41. R. Uecker, D. Klimm, R. Bertram, M. Bernhagen, I. Schulze-Jonack, M. Brützmam, A. Kwasniewski, T.M. Gesing, D.G. Schlom, *Acta Phys. Pol. A* **124**, 295 (2013).
42. A. Lempicki, M.H. Randles, D. Wisniewski, M. Balcerzyk, C. Brecher, A.J. Wojtowicz, *IEEE Trans. Nucl. Sci.* **42**, 280 (1995).
43. A.G. Petrosyan, G.O. Shirinyan, C. Pedrini, C. Durjardin, K.L. Ovanesyan, R.G. Manucharyan, T.I. Butaeva, M.V. Derzyan, *Cryst. Res. Technol.* **33**, 241 (1998).
44. H. Asano, S. Kubo, O. Michikami, M. Satoh, T. Konaka, *Jpn. J. Appl. Phys., Part 2* **29**, L1452 (1990).
45. R. Brown, V. Pendrick, D. Kalokitis, B.H.T. Chai, *Appl. Phys. Lett.* **57**, 1351 (1990).
46. Y. Miyazawa, H. Tushima, S. Morita, *J. Cryst. Growth* **128**, 668 (1993).
47. G.W. Berkstresser, A.J. Valentino, C.D. Brandle, *J. Cryst. Growth* **109**, 467 (1991).
48. G.W. Berkstresser, A.J. Valentino, C.D. Brandle, *J. Cryst. Growth* **128**, 684 (1993).
49. S. Hontsu, J. Ishii, T. Kawai, S. Kawai, *Appl. Phys. Lett.* **59**, 2886 (1991).
50. D. Mateika, H. Kohler, H. Laudan, E. Volkel, *J. Cryst. Growth* **109**, 447 (1991).
51. R.W. Simon, C.E. Platt, A.E. Lee, G.S. Lee, K.P. Daly, M.S. Wire, J.A. Luine, M. Urbanik, *Appl. Phys. Lett.* **53**, 2677 (1988).
52. G.W. Berkstresser, A.J. Valentino, C.D. Brandle, *J. Cryst. Growth* **109**, 457 (1991).
53. B.C. Chakoumakos, D.G. Schlom, M. Urbanik, J. Luine, *J. Appl. Phys.* **83**, 1979 (1998).
54. R.L. Sandstrom, E.A. Giess, W.J. Gallagher, A. Segmüller, E.I. Cooper, M.F. Chisholm, A. Gupta, S. Shinde, R.B. Laibowitz, *Appl. Phys. Lett.* **53**, 1874 (1988).
55. L. Merker, US Patent No. 2,684,910 (27 July 1954).
56. J.G. Bednorz, H.J. Scheel, *J. Cryst. Growth* **41**, 5 (1977).
57. P.I. Nabokin, D. Souptel, A.M. Balbashov, *J. Cryst. Growth* **250**, 397 (2003).
58. H.J. Scheel, J.G. Bednorz, P. Dill, *Ferroelectrics* **13**, 507 (1976).
59. S.-G. Lim, S. Kriventsov, T.N. Jackson, J.H. Haeni, D.G. Schlom, A.M. Balbashov, R. Uecker, P. Reiche, J.L. Freeouf, G. Lucovsky, *J. Appl. Phys.* **91**, 4500 (2002).
60. A. Soukiassian, W. Tian, V. Vaithyanathan, J.H. Haeni, L.Q. Chen, X.X. Xi, D.G. Schlom, D.A. Tenne, H.P. Sun, X.Q. Pan, K.J. Choi, C.B. Eom, Y.L. Li, Q.X. Jia, C. Constantin, R.M. Feenstra, M. Bernhagen, P. Reiche, R. Uecker, *J. Mater. Res.* **23**, 1417 (2008).
61. R. Feenstra, L.A. Boatner, J.D. Budai, D.K. Christen, M.D. Galloway, D.B. Poker, *Appl. Phys. Lett.* **54**, 1063 (1989).
62. J.C. Yang, Q. He, S.J. Suresha, C.Y. Kuo, C.Y. Peng, R.C. Haislmaier, M.A. Motyka, G. Sheng, C. Adamo, H.J. Lin, Z. Hu, L. Chang, L.H. Tjeng, E. Arenholz, N.J. Podraza, M. Bernhagen, R. Uecker, D.G. Schlom, V. Gopalan, L.Q. Chen, C.T. Chen, R. Ramesh, Y.H. Chu, *Phys. Rev. Lett.* **109**, 247606 (2012).
63. S. Coh, T. Heeg, J.H. Haeni, M.D. Biegalski, J. Lettieri, L.F. Edge, K.E. O'Brien, M. Bernhagen, P. Reiche, R. Uecker, S. Trolier-McKinstry, D.G. Schlom, D. Vanderbilt, *Phys. Rev. B* **82**, 064101 (2010).
64. K.L. Ovanesyan, A.G. Petrosyan, G.O. Shirinyan, C. Pedrini, L. Zhang, *J. Cryst. Growth* **198**, 497 (1999).
65. M.D. Biegalski, Y. Jia, D.G. Schlom, S. Trolier-McKinstry, S.K. Streiffer, V. Sherman, R. Uecker, P. Reiche, *Appl. Phys. Lett.* **88**, 192907 (2006).
66. J.F. Ihlefeld, W. Tian, Z.-K. Liu, W.A. Doolittle, M. Bernhagen, P. Reiche, R. Uecker, R. Ramesh, D.G. Schlom, *IEEE Trans. Ultrason. Ferroelectr. Freq. Control* **56**, 1528 (2009).
67. J.H. Lee, X. Ke, R. Misra, J.F. Ihlefeld, X.S. Xu, Z.G. Mei, T. Heeg, M. Roedererath, J. Schubert, Z.K. Liu, J.L. Musfeldt, P. Schiffer, D.G. Schlom, *Appl. Phys. Lett.* **96**, 262905 (2010).
68. P. Irvin, J. Levy, J.H. Haeni, D.G. Schlom, *Appl. Phys. Lett.* **88**, 042902 (2006).
69. H.Z. Ma, J. Levy, M.D. Biegalski, S. Trolier-McKinstry, D.G. Schlom, *J. Appl. Phys.* **105**, 014102 (2009).
70. A. Vasudevarao, A. Kumar, L. Tian, J.H. Haeni, Y.L. Li, C.-J. Klund, Q.X. Jia, R. Uecker, P. Reiche, K.M. Rabe, L.Q. Chen, D.G. Schlom, V. Gopalan, *Phys. Rev. Lett.* **97**, 257602 (2006).
71. A. Vasudevarao, S. Denev, M.D. Biegalski, Y.L. Li, L.Q. Chen, S. Trolier-McKinstry, D.G. Schlom, V. Gopalan, *Appl. Phys. Lett.* **92**, 192902 (2008).
72. S. Denev, A. Kumar, M.D. Biegalski, H.W. Jang, C.M. Folkman, A. Vasudevarao, Y. Han, I.M. Reaney, S. Trolier-McKinstry, C.B. Eom, D.G. Schlom, V. Gopalan, *Phys. Rev. Lett.* **100**, 257601 (2008).
73. M.D. Biegalski, E. Vlahos, G. Sheng, Y.L. Li, M. Bernhagen, P. Reiche, R. Uecker, S.K. Streiffer, L.Q. Chen, V. Gopalan, D.G. Schlom, S. Trolier-McKinstry, *Phys. Rev. B* **79**, 224117 (2009).
74. D. Nuzhnyy, J. Peltzelt, S. Kamba, P. Kužel, C. Kadlec, V. Bovtun, M. Kempa, J. Schubert, C.M. Brooks, D.G. Schlom, *Appl. Phys. Lett.* **95**, 232902 (2009).
75. C.H. Lee, V. Skoromets, M.D. Biegalski, S. Lei, R. Haislmaier, M. Bernhagen, R. Uecker, X.X. Xi, V. Gopalan, X. Martí, S. Kamba, P. Kužel, D.G. Schlom, *Appl. Phys. Lett.* **102**, 082905 (2013).
76. K.J. Hubbard, D.G. Schlom, *J. Mater. Res.* **11**, 2757 (1996).
77. D.G. Schlom, S. Guha, S. Datta, *MRS Bull.* **33**, 1017 (2008).
78. L.F. Kourkoutis, C.S. Hellberg, V. Vaithyanathan, H. Li, M.K. Parker, K.E. Andersen, D.G. Schlom, D.A. Muller, *Phys. Rev. Lett.* **100**, 036101 (2008).
79. H. Li, X. Hu, Y. Wei, Z. Yu, X. Zhang, R. Droopad, A.A. Demkov, J. Edwards, K. Moore, W. Ooms, J. Kulik, P. Fejes, *J. Appl. Phys.* **93**, 4521 (2003).
80. M. Kawasaki, K. Takahashi, T. Maeda, R. Tsuchiya, M. Shinohara, O. Ishiyama, T. Yonezawa, M. Yoshimoto, H. Koinuma, *Science* **266**, 1540 (1994).
81. G. Koster, B.L. Kropman, G.J.H.M. Rijnders, D.H.A. Blank, H. Rogalla, *Appl. Phys. Lett.* **73**, 2920 (1998).
82. A.G. Schrott, J.A. Misewich, M. Copel, D.W. Abraham, Y. Zhang, *Appl. Phys. Lett.* **79**, 1786 (2001).
83. A. Biswas, P.B. Rossen, C.H. Yang, W. Siemons, M.H. Jung, I.K. Yang, R. Ramesh, Y.H. Jeong, *Appl. Phys. Lett.* **98**, 051904 (2011).
84. J. Chang, Y.-S. Park, S.-K. Kim, *Appl. Phys. Lett.* **92**, 152910 (2008).
85. J.L. Blok, X. Wan, G. Koster, D.H.A. Blank, G. Rijnders, *Appl. Phys. Lett.* **99**, 151917 (2011).
86. T. Ohnishi, K. Takahashi, M. Nakamura, M. Kawasaki, M. Yoshimoto, H. Koinuma, *Appl. Phys. Lett.* **74**, 2531 (1999).
87. J.H. Ngai, T.C. Schwendemann, A.E. Walker, Y. Segal, F.J. Walker, E.I. Altman, C.H. Ahn, *Adv. Mater.* **22**, 2945 (2010).
88. J.E. Kleibecker, G. Koster, W. Siemons, D. Dubbink, B. Kuiper, J.L. Blok, C.-H. Yang, J. Ravichandran, R. Ramesh, J.E. ten Elshof, D.H.A. Blank, G. Rijnders, *Adv. Funct. Mater.* **20**, 3490 (2010).
89. J.E. Kleibecker, B. Kuiper, S. Harkema, D.H.A. Blank, G. Koster, G. Rijnders, P. Tinnemans, E. Vlieg, P.B. Rossen, W. Siemons, G. Portale, J. Ravichandran, J.M. Szeplieniec, R. Ramesh, *Phys. Rev. B* **85**, 165413 (2012).
90. H.-J. Bae, J. Sigman, D.P. Norton, L.A. Boatner, *Appl. Surf. Sci.* **241**, 271 (2005).
91. N.A. Pertsev, A.G. Zembilgotov, A.K. Tagantsev, *Phys. Rev. Lett.* **80**, 1988 (1998).
92. O. Diéguez, S. Tinte, A. Antons, C. Bungaro, J.B. Neaton, K.M. Rabe, D. Vanderbilt, *Phys. Rev. B* **69**, 212101 (2004).
93. Y.L. Li, L.Q. Chen, *Appl. Phys. Lett.* **88**, 072905 (2006).
94. D.A. Tenne, P. Turner, J.D. Schmidt, M. Biegalski, Y.L. Li, L.Q. Chen, A. Soukiassian, S. Trolier-McKinstry, D.G. Schlom, X.X. Xi, D.D. Fong, P.H. Fuoss, J.A. Eastman, G.B. Stephenson, C. Thompson, S.K. Streiffer, *Phys. Rev. Lett.* **103**, 177601 (2009).
95. A. Pertsev, V.G. Koukhar, *Phys. Rev. Lett.* **84**, 3722 (2000).
96. V.G. Koukhar, N.A. Pertsev, R. Waser, *Phys. Rev. B* **64**, 214103 (2001).
97. Y.L. Li, S.Y. Hu, Z.K. Liu, L.Q. Chen, *Appl. Phys. Lett.* **78**, 3878 (2001).
98. Y.L. Li, S.Y. Hu, Z.K. Liu, L.Q. Chen, *Acta Mater.* **50**, 395 (2002).
99. S.K. Streiffer, J.A. Eastman, D.D. Fong, C. Thompson, A. Munkholm, M.V.R. Murty, O. Auciello, G.R. Bai, G.B. Stephenson, *Phys. Rev. Lett.* **89**, 067601 (2002).
100. D.D. Fong, G.B. Stephenson, S.K. Streiffer, J.A. Eastman, O. Auciello, P.H. Fuoss, C. Thompson, *Science* **304**, 1650 (2004).
101. K. Abe, N. Yanase, K. Sano, M. Izuha, N. Fukushima, T. Kawakubo, *Integr. Ferroelectr.* **21**, 197 (1998).
102. N. Yanase, K. Abe, N. Fukushima, T. Kawakubo, *Jpn. J. Appl. Phys., Part 1* **38**, 5305 (1999).
103. E.D. Specht, H.-M. Christen, D.P. Norton, L.A. Boatner, *Phys. Rev. Lett.* **80**, 4317 (1998).
104. H.-M. Christen, L.A. Krauss, K.S. Harshavardhan, *Mater. Sci. Eng., B* **56**, 200 (1998).
105. H.-M. Christen, E.D. Specht, S.S. Silliman, K.S. Harshavardhan, *Phys. Rev. B* **68**, 20101 (2003).
106. M. Dawber, C. Lichtensteiger, M. Cantoni, M. Veithen, P. Ghosez, K. Johnston, K.M. Rabe, J.-M. Triscone, *Phys. Rev. Lett.* **95**, 177601 (2005).
107. E. Bousquet, M. Dawber, N. Stucki, C. Lichtensteiger, P. Hermet, S. Gariglio, J.M. Triscone, P. Ghosez, *Nature* **452**, 732 (2008).
108. J.B. Neaton, K.M. Rabe, *Appl. Phys. Lett.* **82**, 1586 (2003).
109. D.A. Tenne, A. Bruchhausen, N.D. Lanzillotti-Kimura, A. Fainstein, R.S. Katiyar, A. Cantarero, A. Soukiassian, V. Vaithyanathan, J.H. Haeni, W. Tian, D.G. Schlom, K.J. Choi, D.M. Kim, C.B. Eom, H.P. Sun, X.Q. Pan, Y.L. Li, L.Q. Chen, Q.X. Jia, S.M. Nakhmanson, K.M. Rabe, X.X. Xi, *Science* **313**, 1614 (2006).
110. Y.L. Li, S.Y. Hu, D. Tenne, A. Soukiassian, D.G. Schlom, X.X. Xi, K.J. Choi, C.B. Eom, A. Saxena, T. Lookman, Q.X. Jia, L.Q. Chen, *Appl. Phys. Lett.* **91**, 112914 (2007).
111. Y.L. Li, S.Y. Hu, D. Tenne, A. Soukiassian, D.G. Schlom, L.Q. Chen, X.X. Xi, K.J. Choi, C.B. Eom, A. Saxena, T. Lookman, Q.X. Jia, *Appl. Phys. Lett.* **91**, 252904 (2007).
112. N. Sai, B. Meyer, D. Vanderbilt, *Phys. Rev. Lett.* **84**, 5636 (2000).
113. M.R. Warusawithana, E.V. Colla, J.N. Eckstein, M.B. Weissman, *Phys. Rev. Lett.* **90**, 036802 (2003).
114. H.N. Lee, H.M. Christen, M.F. Chisholm, C.M. Rouleau, D.H. Lowndes, *Nature* **433**, 395 (2005).
115. A.G. Zembilgotov, N.A. Pertsev, U. Böttger, R. Waser, *Appl. Phys. Lett.* **86**, 052903 (2005).

116. G. Sheng, Y.L. Li, J.X. Zhang, S. Choudhury, Q.X. Jia, V. Gopalan, D.G. Schlom, Z.K. Liu, L.Q. Chen, *J. Appl. Phys.* **108**, 084113 (2010).
117. K. Kathan-Galipeau, P.P. Wu, Y.L. Li, L.Q. Chen, A. Soukiassian, X.X. Xi, D.G. Schlom, D.A. Bonnelli, *ACS Nano* **5**, 640 (2011).
118. K. Kathan-Galipeau, P.P. Wu, Y.L. Li, L.Q. Chen, A. Soukiassian, Y. Zhu, D.A. Muller, X.X. Xi, D.G. Schlom, D.A. Bonnelli, *J. Appl. Phys.* **112**, 052011 (2012).
119. J. Ravichandran, A.K. Yadav, R. Cheaito, P.B. Rossen, A. Soukiassian, S.J. Suresha, J.C. Duda, B.M. Foley, C.H. Lee, Y. Zhu, A.W. Lichtenberger, J.E. Moore, D.A. Muller, D.G. Schlom, P.E. Hopkins, A. Majumdar, R. Ramesh, M.A. Zurbuchen, *Nat. Mater.* (2013), in press, doi: 10.1038/nmat3826.
120. J. Wang, J.B. Neaton, H. Zheng, V. Nagarajan, S.B. Ogale, B. Liu, D. Viehland, V. Vaithyanathan, D.G. Schlom, U.V. Waghmare, N.A. Spaldin, K.M. Rabe, M. Wuttig, R. Ramesh, *Science* **299**, 1719 (2003).
121. R. Ramesh, N.A. Spaldin, *Nat. Mater.* **6**, 21 (2007).
122. A.A. Belik, S. Iikubo, K. Kodama, N. Igawa, S.-I. Shamoto, S. Niitaka, M. Azuma, Y. Shimakawa, M. Takano, F. Izumi, E. Takayama-Muromachi, *Chem. Mater.* **18**, 798 (2006).
123. M.-R. Li, U. Adem, S.R.C. McMitchell, Z. Xu, C.I. Thomas, J.E. Warren, D.V. Giap, H. Niu, X. Wan, R.G. Palgrave, F. Schiffrmann, F. Cora, B. Slater, T.L. Burnett, M.G. Cain, A.M. Abakumov, G. van Tendeloo, M.F. Thomas, M.J. Rosseinsky, J.B. Claridge, *J. Am. Chem. Soc.* **134**, 3737 (2012).
124. W. Wang, J. Zhao, W. Wang, Z. Gai, N. Balke, M. Chi, H.N. Lee, W. Tian, L. Zhu, X. Cheng, D.J. Keavney, J. Yi, T.Z. Ward, P.C. Snijders, H.M. Christen, W. Wu, J. Shen, X. Xu, *Phys. Rev. Lett.* **110**, 237601 (2013).
125. J.F. Li, J. Wang, M. Wuttig, R. Ramesh, N. Wang, B. Ruetter, A.P. Pyatakov, A.K. Zvezdin, D. Viehland, *Appl. Phys. Lett.* **84**, 5261 (2004).
126. R.R. Das, D.M. Kim, S.H. Baek, C.B. Eom, F. Zavaliche, S.Y. Yang, R. Ramesh, Y.B. Chen, X.Q. Pan, X. Ke, M.S. Rzchowski, S.K. Streiffer, *Appl. Phys. Lett.* **88**, 242904 (2006).
127. J. Dho, X. Qi, H. Kim, J.L. MacManus-Driscoll, M.G. Blamire, *Adv. Mater.* **18**, 1445 (2006).
128. F. Kubel, H. Schmid, *Acta Crystallogr., Sect. B: Struct. Sci.* **46**, 698 (1990).
129. A.J. Hatt, N.A. Spaldin, C. Ederer, *Phys. Rev. B* **81**, 054109 (2010).
130. A.G. Christy, *Acta Crystallogr. Sect. B: Struct. Sci.* **51**, 753 (1995).
131. L. Ehm, K. Knorr, L. Peters, S. Rath, W. Depmeier, *J. Alloys Compd.* **429**, 82 (2007).
132. J. Haines, J.M. Léger, O. Schulte, *Phys. Rev. B* **57**, 7551 (1998).
133. J.X. Zhang, B. Xiang, Q. He, J. Seidel, R.J. Zeches, P. Yu, S.Y. Yang, C.H. Wang, Y.H. Chu, L.W. Martin, A.M. Minor, R. Ramesh, *Nat. Nanotechnol.* **6**, 98 (2011).
134. Q. He, Y.H. Chu, J.T. Heron, S.Y. Yang, W.I. Liang, C.Y. Kuo, H.J. Lin, P. Yu, C.W. Liang, R.J. Zeches, W.C. Kuo, J.Y. Juang, C.T. Chen, E. Arenholz, A. Scholl, R. Ramesh, *Nat. Commun.* **2**, 225 (2011).
135. J.C. Yang, Q. He, S.J. Suresha, C.Y. Kuo, C.Y. Peng, R.C. Haismaier, M.A. Motyka, G. Sheng, C. Adamo, H.J. Lin, Z. Hu, L. Chang, L.H. Tjeng, E. Arenholz, N.J. Podraza, M. Bernhagen, R. Uecker, D.G. Schlom, V. Gopalan, L.Q. Chen, C.T. Chen, R. Ramesh, Y.H. Chu, *Phys. Rev. Lett.* **109**, 247606 (2012).
136. C.J. Fennie, K.M. Rabe, *Phys. Rev. Lett.* **97**, 267602 (2006).
137. J.P. Rivera, H. Schmid, *Ferroelectrics* **36**, 447 (1981).
138. W. von Wartburg, *Phys. Status Solidi A* **21**, 557 (1974).
139. T. Birol, C.J. Fennie, *Phys. Rev. B* **88**, 094103 (2013).
140. T.R. McGuire, M.W. Shafer, R.J. Joenk, H.A. Alperin, S.J. Pickart, *J. Appl. Phys.* **37**, 981 (1966).
141. C.-L. Chien, S. DeBenedetti, F. De S. Barros, *Phys. Rev. B* **10**, 3913 (1974).
142. T. Katsufuji, H. Takagi, *Phys. Rev. B* **64**, 054415 (2001).
143. H.-H. Wang, A. Fleet, J.D. Brock, D. Dale, Y. Suzuki, *J. Appl. Phys.* **96**, 5324 (2004).
144. K. Kugimiya, K. Fujita, K. Tanaka, K. Hirao, *J. Magn. Magn. Mater.* **310**, 2268 (2007).
145. S.C. Chae, Y.J. Chang, D.-W. Kim, B.W. Lee, I. Choi, C.U. Jung, *J. Electroceram.* **22**, 216 (2009).
146. K. Fujita, N. Wakasugi, S. Murai, Y. Zong, K. Tanaka, *Appl. Phys. Lett.* **94**, 062512 (2009).
147. M.W. Schafer, *J. Appl. Phys.* **36**, 1145 (1965).
148. G.J. McCarthy, W.B. White, R. Roy, *J. Inorg. Nucl. Chem.* **31**, 329 (1969).
149. Y.S. Kim, D.J. Kim, T.H. Kim, T.W. Noh, J.S. Choi, B.H. Park, J.-G. Yoon, *Appl. Phys. Lett.* **91**, 042908 (2007).
150. K.A. Müller, H. Burkard, *Phys. Rev. B* **19**, 3593 (1979).
151. E.J. Tarsa, E.A. Hachfeld, F.T. Quinlan, J.S. Speck, M. Eddy, *Appl. Phys. Lett.* **68**, 490 (1996).
152. T. Ohnishi, M. Lippmaa, T. Yamamoto, S. Meguro, H. Koinuma, *Appl. Phys. Lett.* **87**, 2419191 (2005).
153. T. Ohnishi, K. Shibuya, T. Yamamoto, M. Lippmaa, *J. Appl. Phys.* **103**, 103703 (2008).
154. M. Kestigian, J.G. Dickinson, R. Ward, *J. Am. Chem. Soc.* **79**, 5598 (1957).
155. D.A. Tenne, I.E. Gonenli, A. Soukiassian, D.G. Schlom, S.M. Nakhmanson, K.M. Rabe, X.X. Xi, *Phys. Rev. B* **76**, 024303 (2007).
156. C.M. Brooks, L. Fitting Kourkoutis, T. Heeg, J. Schubert, D.A. Muller, D.G. Schlom, *Appl. Phys. Lett.* **94**, 162905 (2009).
157. J.H. Lee, X. Ke, N.J. Podraza, L. Fitting Kourkoutis, T. Heeg, M. Roeckerath, J.W. Freeland, C.J. Fennie, J. Schubert, D.A. Muller, P. Schiffer, D.G. Schlom, *Appl. Phys. Lett.* **94**, 212509 (2009).
158. J.H. Lee, K.M. Rabe, *Phys. Rev. Lett.* **104**, 207204 (2010).
159. E. Bousquet, N.A. Spaldin, P. Ghosez, *Phys. Rev. Lett.* **104**, 037601 (2010).
160. P.J. Ryan, J.-W. Kim, T. Birol, P. Thompson, J.-H. Lee, X. Ke, P.S. Normile, E. Karapetrova, P. Schiffer, S.D. Brown, C.J. Fennie, D.G. Schlom, *Nat. Commun.* **4**, 1334 (2013).
161. C.H. Lee, N.D. Orloff, T. Birol, Y. Zhu, V. Goian, E. Rocas, R. Haismaier, E. Vlahos, J.A. Mundy, L.F. Kourkoutis, Y. Nie, M.D. Biegalski, J. Zhang, M. Bernhagen, N.A. Benedek, Y. Kim, J.D. Brock, R. Uecker, X.X. Xi, V. Gopalan, D. Nuzhnyy, S. Kamba, D.A. Muller, I. Takeuchi, J.C. Booth, C.J. Fennie, D.G. Schlom, *Nature* **502**, 532 (2013).
162. O.G. Vendik, *Ferroelectrics* **12**, 85 (1976).
163. S.W. Kirchoefer, J.M. Pond, A.C. Carter, W. Chang, K.K. Agarwal, J.S. Horwitz, D.B. Chrisey, *Microwave Opt. Technol. Lett.* **18**, 168 (1998).
164. S.S. Gevorgian, E.L. Kollberg, *IEEE Trans. Microwave Theory Tech.* **49**, 2117 (2001).
165. A.K. Tagantsev, V.O. Sherman, K.F. Astafiev, J. Venkatesh, N. Setter, *J. Electroceram.* **11**, 5 (2003).
166. S. Andersson, A.D. Wadsley, *Nature* **211**, 581 (1966).
167. J.S. Anderson, J.M. Browne, A.K. Cheetham, R. Vondree, J.L. Hutchison, F.J. Lincoln, D.J.M. Bevan, J. Straehle, *Nature* **243**, 81 (1973).
168. R.J.D. Tilley, *Nature* **269**, 229 (1977).
169. R.J.D. Tilley, *J. Solid State Chem.* **21**, 293 (1977).
170. T. Nakamura, P.H. Sun, Y.J. Shan, Y. Inaguma, M. Itoh, I.S. Kim, J.H. Sohn, M. Ikeda, T. Kitamura, H. Konagaya, *Ferroelectrics* **196**, 205 (1997).
171. P.L. Wise, I.M. Reaney, W.E. Lee, T.J. Price, D.M. Iddles, D.S. Cannell, *J. Eur. Ceram. Soc.* **21**, 1723 (2001).
172. N.D. Orloff, W. Tian, C.J. Fennie, C.H. Lee, D. Gu, J. Mateu, X.X. Xi, K.M. Rabe, D.G. Schlom, I. Takeuchi, J.C. Booth, *Appl. Phys. Lett.* **94**, 042908 (2009).
173. T. Birol, N.A. Benedek, C.J. Fennie, *Phys. Rev. Lett.* **107**, 257602 (2011).
174. D.O. Klenov, W. Donner, B. Foran, S. Stemmer, *Appl. Phys. Lett.* **82**, 3427 (2003).
175. W. Donner, C. Chen, M. Liu, A.J. Jacobson, Y.-L. Lee, M. Gadre, D. Morgan, *Chem. Mater.* **23**, 984 (2011).
176. J.M. Rondinelli, N.A. Spaldin, *Adv. Mater.* **23**, 3363 (2011).
177. J.M. Rondinelli, S.J. May, J.W. Freeland, *MRS Bull.* **37**, 261 (2012).
178. W.S. Choi, J.-H. Kwon, H. Jeon, J.E. Hamann-Borrero, A. Radi, S. Macke, R. Sutarto, F. He, G.A. Sawatzky, V. Hinkov, M. Kim, H.N. Lee, *Nano Lett.* **12**, 4966 (2012).
179. Y. Yang, C.M. Schlepütz, C. Adamo, D.G. Schlom, R. Clarke, *APL Mater.* **1**, 052102 (2013).
180. C.-L. Jia, V. Nagarajan, J.-Q. He, L. Houben, T. Zhao, R. Ramesh, K. Urban, R. Waser, *Nat. Mater.* **6**, 64 (2006).
181. C.-L. Jia, S.-B. Mi, K. Urban, I. Vrejoiu, M. Alexe, D. Hesse, *Nat. Mater.* **7**, 57 (2008).
182. C.T. Nelson, B. Winchester, Y. Zhang, S.-J. Kim, A. Melville, C. Adamo, C.M. Folkman, S.-H. Baek, C.-B. Eom, D.G. Schlom, L.-Q. Chen, X. Pan, *Nano Lett.* **11**, 828 (2011).
183. C.L. Jia, K.W. Urban, M. Alexe, D. Hesse, I. Vrejoiu, *Science* **331**, 1420 (2011).
184. A.Y. Borisevich, H.J. Chang, M. Huijben, M.P. Oxley, S. Okamoto, M.K. Niranjan, J.D. Burton, E.Y. Tsybmal, Y.H. Chu, P. Yu, R. Ramesh, S.V. Kalinin, S.J. Pennycook, *Phys. Rev. Lett.* **105**, 087204 (2010).
185. D.A. Muller, L.F. Kourkoutis, M. Murfitt, J.H. Song, H.Y. Hwang, J. Silcox, N. Dellby, O.L. Krivanek, *Science* **319**, 1073 (2008).
186. D. Lee, R. Behera, P. Wu, H. Xu, Y.L. Li, S.B. Sinnott, S. Phillpot, L. Chen, V. Gopalan, *Phys. Rev. B* **80**, 060102 (2009).
187. E.F. Kneller, R. Hawig, *Magnetics, IEEE Trans. Magn.* **27**, 3588 (1991).
188. E.E. Fullerton, J.S. Jiang, S.D. Bader, *J. Magn. Magn. Mater.* **200**, 392 (1999).
189. P. Wu, X. Ma, Y. Li, V. Gopalan, L.Q. Chen, *Appl. Phys. Lett.* **100**, 092905 (2012).
190. J.H. Lee, K.M. Rabe, *Phys. Rev. Lett.* **107**, 067601 (2011).
191. D.M. Newsn, B.G. Elmegreen, X.-H. Liu, G.J. Martyna, *Adv. Mater.* **24**, 3672 (2012).
192. D. Newsn, B. Elmegreen, X. Hu Liu, G. Martyna, *J. Appl. Phys.* **111**, 084509 (2012).
193. R.E. Newnham, J.J. Kramer, W.A. Schulze, L.E. Cross, *J. Appl. Phys.* **49**, 6088 (1978).
194. M.J. Harris, S.T. Bramwell, D.F. McMorrow, T. Zeiske, K.W. Godfrey, *Phys. Rev. Lett.* **79**, 2554 (1997).

195. C. Fennie, K. Rabe, *Phys. Rev. B* **72**, 100103 (2005).
 196. T. Choi, Y. Horibe, H.T. Yi, Y.J. Choi, W. Wu, S.W. Cheong, *Nat. Mater.* **9**, 253 (2010).
 197. A. Arkenbout, T. Palstra, T. Siegrist, T. Kimura, *Phys. Rev. B* **74**, 184431 (2006).
 198. F. Ye, Y. Ren, Q. Huang, J. Fernandez-Baca, P. Dai, J. Lynn, T. Kimura, *Phys. Rev. B* **73**, 220404 (2006).
 199. T. Kimura, Y. Sekio, H. Nakamura, T. Siegrist, A.P. Ramirez, *Nat. Mater.* **7**, 291 (2008).
 200. Y. Kitagawa, Y. Hiraoka, T. Honda, T. Ishikura, H. Nakamura, T. Kimura, *Nat. Mater.* **9**, 797 (2010).
 201. A.A. Bossak, I.E. Graboy, O.Y. Gorbenko, A.R. Kaul, M.S. Kartavtseva, V.L. Svetchnikov, H.W. Zandbergen, *Chem. Mater.* **16**, 1751 (2004).
 202. W. Wang, J. Zhao, W. Wang, Z. Gai, N. Balke, M. Chi, H.N. Lee, W. Tian, L. Zhu, X. Cheng, D.J. Keavney, J. Yi, T.Z. Ward, P.C. Snijders, H.M. Christen, W. Wu, J. Shen, X. Xu, *Phys. Rev. Lett.* **110**, 237601 (2013).
 203. E.S. Machlin, P. Chaudhari, in *Synthesis and Properties of Metastable Phases*, E.S. Machlin, T.J. Rowland, Eds. (The Metallurgical Society of AIME, Warrendale, 1980), pp. 11–29.
 204. C.P. Flynn, *Phys. Rev. Lett.* **57**, 599 (1986).
 205. R. Bruinsma, A. Zangwill, *J. Phys. (Paris)* **47**, 2055 (1986).
 206. O.Y. Gorbenko, S.V. Samoilenkov, I.E. Graboy, A.R. Kaul, *Chem. Mater.* **14**, 4026 (2002).
 207. J.M. Rondinelli, C.J. Fennie, *Adv. Mater.* **24**, 1961 (2012).
 208. A.T. Mulder, N.A. Benedek, J.M. Rondinelli, C.J. Fennie, *Adv. Funct. Mater.* **23**, 4810 (2013).
 209. C.J. Fennie, *Phys. Rev. Lett.* **100**, 167203 (2008).
 210. T. Varga, A. Kumar, E. Vlahos, S. Denev, M. Park, S. Hong, T. Sanehira, Y. Wang, C. Fennie, S. Streiffner, X. Ke, P. Schiffer, V. Gopalan, J. Mitchell, *Phys. Rev. Lett.* **103**, 047601 (2009).
 211. G. Singh-Bhalla, C. Bell, J. Ravichandran, W. Siemons, Y. Hikita, S. Salahuddin, A.F. Hebard, H.Y. Hwang, R. Ramesh, *Nat. Phys.* **7**, 80 (2010). □

Career Center

JOB SEEKERS MEET YOUR NEXT EMPLOYER!

We'll show off your talents to the world's most prestigious high-tech firms, universities and laboratories. At the 2014 MRS Spring Meeting Career Center, you can access many interesting job postings, visit recruitment booths and interview with prospective employers. Please bring extra copies of your resume for your own use.

The Career Center is FREE to all MRS members and those registered to attend the 2014 MRS Spring Meeting.


ON-SITE REGISTRATION HOURS
 Monday, April 21 1:00 pm – 4:00 pm
 (Candidate Registration Only)

CAREER CENTER HOURS
 Tuesday, April 22 10:00 am – 5:00 pm
 Wednesday, April 23 10:00 am – 5:00 pm

Register and submit your resume today!


www.mrs.org/spring-2014-career-center

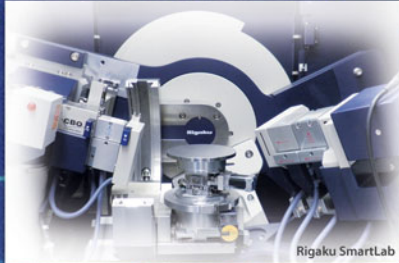




Rigaku

Better measurements. Better confidence. Better world.





Rigaku SmartLab

www.Rigaku.com/products/xrd/smartlab

Powder Diffraction • Thin Film Diffraction • SAXS • In-Plane Grazing Incidence

Rigaku's SmartLab® is the most versatile diffractometer in the world. You can start using all XRD applications from the very first day because of the unique knowledge-based Guidance control software. The available 9 kW line focus X-ray source provides ultimate power for the most demanding applications. Automatic self-alignment ensures that you always collect the best data possible and beam path selection can be made without touching a multilayer optic.

for Material Scientists

The SmartLab combined with a novel two-dimensional detector enables one to measure a large-area reciprocal space map in minutes rather than days.

Rigaku Corporation and its Global Subsidiaries | www.Rigaku.com | info@Rigaku.com